Mike Mann

Ref 11
NASA SMF-2 report

ERR-FW-1940
COSATI Field 20:
Physics
Brochure Project
No. 78006625

11

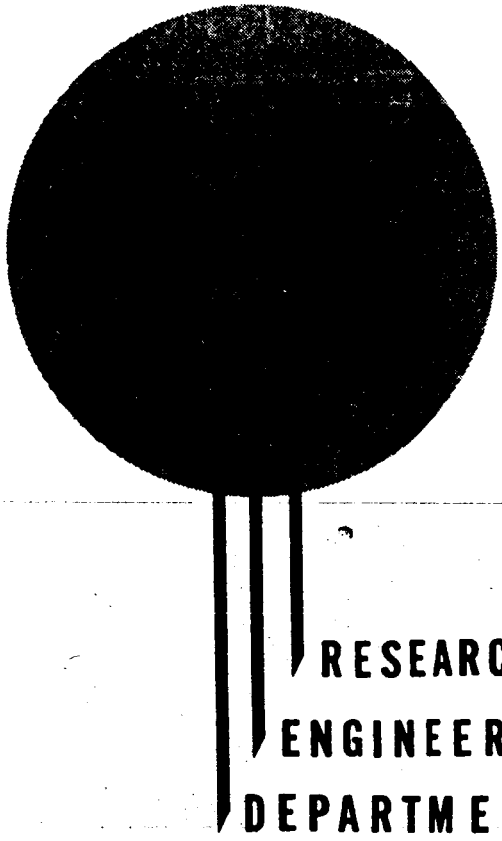

STATUS REPORT ON THE DEVELOPMENT OF A SUPERCRITICAL SLOPED ROOFTOP WING

S. K. HADLEY
H. W. MANN

22 December 1978

Most up to date of 2 GD reports – compare W18 and SMF-1

RESEARCH & ENGINEERING DEPARTMENTS

Note: Dec 78 Astro & Aero pg 53 – Dick Bradley published at M=.90 drag polar on SMF-1 and W18

GENERAL DYNAMICS
Fort Worth Division
P. O. Box 748, Fort Worth, Texas 76101

#140898

ERR-FW-1940
COSATI Field 20:
Physics
Brochure Project No. 78006625

RESEARCH REPORT

STATUS REPORT ON THE DEVELOPMENT OF A SUPERCRITICAL SLOPED ROOFTOP WING

S. K. HADLEY
H. W. MANN

22 DECEMBER 1978

RESEARCH & ENGINEERING DEPARTMENTS

GENERAL DYNAMICS
Fort Worth Division
P. O. Box 748, Fort Worth, Texas 76101

This work was supported by the General Dynamics Research Fund, RDP Task No. 414-85-571.

GENERAL DYNAMICS
Fort Worth Division

CATEGORY OF EFFORT
COSATI Field 01:

Abstract

BROCHURE PROJECT NO. 78006625

REPORT NUMBER ERR-FW-1940 RDP TASK NO. 414-85-571

REPORT TITLE: Status Report on the Development of a Supercritical Sloped Rooftop Wing

AUTHOR(S): S.K. Hadley, H.W. Mann

DATE OF PUBLICATION: 22 December 1978

SECURITY CLASSIFICATION None COMPANY CLASSIFICATION None

The status of a joint NASA and General Dynamics effort to design a supercritical "sloped rooftop" wing is reported. The SMF-1 wing was the result of an extensive theoretical design effort using available transonic computer codes. The Garabedian and Korn 2-D viscous procedure was used to define the airfoil shape that produced the desired "sloped rooftop" pressure distribution. The 3-D Jameson procedure was used to define the spanwise wing contour that would preserve the desired distribution along the wing span. The SMF-1 wing was tested and was found to offer a 7% increase in sustained lift over conventional hinged flaps. The SMF-1 wing also had less drag creep and higher C_L's before the onset of buffet than a previously tested variable camber wing. An analysis of pressure data and oil flow photographs on the SMF-1 indicated that trailing-edge flow separation was limiting the aerodynamic improvements. Attempts to delay this phenomena by altering the trailing-edge camber and by using upper surface vortex generators proved to be unsuccessful.

No. of Pages 49 No. of Figs. 35 No. of Refs. 8 No. of Tables 1

Descriptors:

Fluid Mechanics, Transonic Flow, Supercritical Wing Design, Air-Superiority Fighter, Variable Camber

ACKNOWLEDGEMENT

This project was a joint NASA/General Dynamics effort. Many of the model parts and all of the wind tunnel time were supplied by the NASA Langley Research Center as part of their fighter wing development project. Photographs in this report are reproduced from NASA originals. This research effort was made possible by the generous support of the Transonic Aerodynamics Branch and Fluid Dynamics Branch of NASA/LRC.

TABLE OF CONTENTS

PAGE VI INTENTIONALLY BLANK

LIST OF FIGURES AND TABLES

NOTATION

A	Aspect ratio (b^2/S_{REF})
b	Span
c	Chord
C_R	Root chord
C_{RMS}	Wing bending moment coefficient
C_T	Tip chord
C_D	Drag coefficient
C_l	Section lift coefficient
C_L	Lift coefficient
C_P	Static pressure coefficient
L/D	Lift to drag ratio
M	Mach number
t	Total thickness
S_{REF}	Wing reference area
x/c	Nondimensional chord station
y/c	Nondimensional airfoil ordinate
α	Angle of attack
η	Nondimensional semispan
λ	Taper ratio (C_T/C_R)
Λ	Wing sweep angle
θ	Isobar sweepback angle

SUMMARY

NASA's Langley Research Center and General Dynamics have jointly conducted investigations of advanced fighter wing concepts since 1973. The design philosophy used in these joint investigations has been to obtain the best possible transonic maneuver capability from low-aspect-ratio fighter wings that have thin airfoils in order to preserve good supersonic acceleration. The design and test of a supercritical "sloped-rooftop" concept is presented within this report.

The design of the SMF-1 wing progressed in three stages. These stages were the (1) selection of a planform, (2) design of the airfoil shape, and (3) design of the wing spanwise contour variations. A planform was selected that was capable of producing a design lift coefficient of 0.90 without buffet at Mach 0.90. The airfoil shape that could produce the desired "sloped-rooftop" chordwise pressure distribution was designed with the 2-d viscous Garabedian and Korn procedure. The spanwise variations in camber and twist required to preserve the desired pressure distribution along the wing span were designed with the 3-D Jameson procedure.

Test results on the SMF-1 wing on a NASA fuselage indicated significant aerodynamic improvements. An improvement in sustained lift at $C_{T_{MAX}}$ of the F-100 engine was found for the SMF-1 over a variable-camber wing previously developed jointly by NASA and General Dynamics. This improvement was approximately 7% better than

conventional hinged flaps on a similar planform. This SMF-1 wing also had less drag creep and higher C_L's before the onset of buffet than the previous variable camber wing .

An analysis of pressure data and oil flow photographs on the SMF-1 wing indicated that trailing-edge flow separation was limiting the aerodynamic improvements. Attempts to delay this separation by use of vortex generators and by altering the trailing-edge camber were unsuccessful.

Further refinement of the theoretical design process used for the SMF-1 wing is warranted because of the favorable test results. The wing pressure data indicated that a true "sloped rooftop" distribution was not achieved. More recently developed transonic computer codes need to be evaluated to determine their usefulness for transonic wing design.

The success of the SMF-1 wing can be attributed to its favorable combination of camber and twist. Verification of the favorable effects of the airfoil shape alone is needed to validate the usefulness of the "sloped-rooftop" concept. This suggests testing of an untwisted wing in addition to the wing with optimum twist. The supersonic penalties associated with the required twist also need to be identified.

1. INTRODUCTION

Since initiation in 1973 of a joint NASA/General Dynamics program of research in advanced fighter wing concepts, several transonic technology concepts have been investigated. These experimental investigations were primarily concerned with thin wings of moderate aspect ratio (3 to 4) and leading-edge sweep (30 to 55 degrees). Variable-contour camber was one such concept that indicated a potential improvement in transonic maneuver capability and was reported in References 1-5.

A variable-camber wing labeled W_{18} was experimentally developed in cooperation with Ted Ayers of NASA Langley Research Center in the Langley 8-foot tunnel. The design philosophy was to start with a thin, flat wing for good supersonic characteristics and to provide the capability for variable camber in the leading- and trailing-edge regions. The contoured flap segments for wing W_{18} had been experimentally optimized for high transonic maneuver in the cambered configuration at discrete Mach numbers (Ref. 4).

The experimental investigations with wing W_{18} and similar variable contour wings failed to show sufficiently compelling aerodynamic improvements to justify the added mechanical complexity of a variable contour maneuver flap system (Ref. 5). For this reason, it was decided in 1976 to begin a different approach to the transonic wing design problem. The use of variable camber was not discarded,

but the previous design restrictions (i.e., variable camber restricted to leading- and trailing-edge regions) had to be removed if more sizable improvements were to be found. The process of experimentally developing the desired contour shapes had also proven to be time consuming, expensive, and difficult.

Recent developments in viscous flow computer procedures appeared to be an attractive addition to the experimental "tuning" process used to design previous variable camber wings. If these theoretical procedures could be used to define the chordwise and spanwise camber variations that would produce the flow properties desired by the aerodynamicist, the experimental phase could be used to verify and final tune the wing aerodynamic characteristics. With this in mind a cooperative NASA/General Dynamics wing design was initiated in 1976. The resulting wing design, which was designated SMF-1 (Supercritical Maneuver Fighter Wing), was reported in Reference 6. This report reviews the design of the SMF-1 wing and documents the significant experimental results obtained to date.

2. REVIEW OF SMF-1 WING DESIGN

One of the goals that aerodynamicists strive for in transonic wing designs is the prevention, delay, or control of the formation of drag- and buffet-producing shocks. The concept of the "sloped-rooftop" wing was a wing shape which produces a chordwise, sloped pressure distribution that allows the flow to reach the critical flow conditions over the entire surface without creating a strong shock. Ideally this type of pressure distribution allows the wing to generate its maximum lift load before shock-induced separation and the associated increase in profile drag occur. The result would be a wing with superior transonic maneuverability characteristics.

As reported in Reference 6, the design of the "sloped-rooftop" supercritical wing proceeded in three phases: planform development, airfoil development, and wing contour development. A thin wing (t/c=.0425) that could produce a lift coefficient of 0.90 without inducing buffet at Mach 0.90 was the design criteria for selection of a wing planform.

By defining the desired static pressure distribution corresponding to critical flow conditions (i.e., local Mach number = 1.0), as shown in Figure 1, and integrating this distribution over the wing planform, it can be shown that the design lift coefficient

EQUATIONS USED TO DEVELOP SUPERCRITICAL PRESSURE DISTRIBUTION

$$\tan \Lambda_{t\,x/c} = \tan \Lambda_{le} - \frac{4(x/c)}{AR}\left(\frac{1-\lambda}{1+\lambda}\right)$$

$$\theta_{ISOBAR} = \Lambda_{LOCAL}$$

$$\text{LOCAL SONIC } C_p = \frac{2}{\gamma M^2 \cos^2\theta}\left[\left[\frac{1+\frac{\gamma-1}{2}M^2\cos^2\theta}{1+\frac{\gamma-1}{2}}\right]^{\frac{\gamma}{\gamma-1}} - 1\right]$$

$$\int_0^1 C_{p,\,thickness}\, d(x/c) = 2.37\,(t/c)$$

$$C_l = 2\int \left[C_{p,\,upper\ surface} - C_{p,\,thickness}\right] d(x/c)$$

$$C_l^* = C_{l,\,critical} + \Delta C_{l,\,supercritical}$$

$$= C_{l,\,critical} + 0.26$$

TARGET UPPER SURFACE PRESSURE DISTRIBUTION

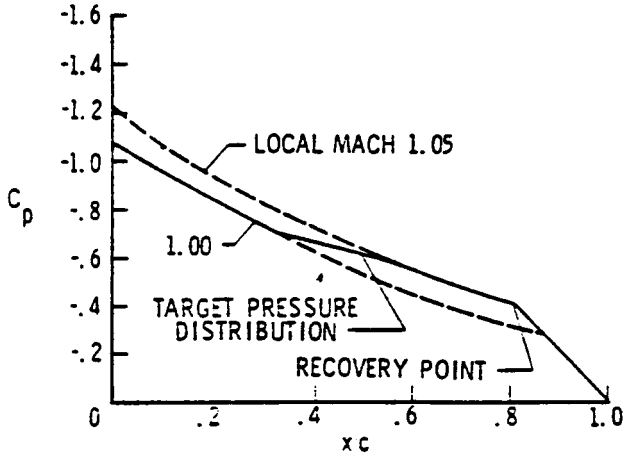

Figure 1 - Target 2-D Upper Surface Pressure Distribution

is a function of the planform shape (i.e., $\mathcal{R}$, λ , and Λ), t/c, and M_∞ . Therefore, the planform shapes that are capable of producing a buffet free lift coefficient of 0.90 at a freestream Mach number of 0.9 can be defined as shown in Figure 2 for a thin wing. It is interesting to note in Figure 2 that a family of forward swept wings which can potentially develop the design lift coefficient ,is defined in addition to the conventional aft swept wings.

The planform selected for the SMF-1 wing design had an aspect ratio of 3.28, taper ratio of 0.2142, and leading-edge sweep angle of 45 deg.This planform shown in Figure 3 was selected because it was a typical fighter type planform, it fell within the parametric family of desired planforms defined in Figure 2, and it was compatible with the variable camber wings previously tested as discussed in Reference 6.

With the desired pressure distribution defined as shown in Figure 1 and the planform shape selected as shown in Figure 3, the next phase of the SMF-1 wing design was the definition of an airfoil shape that could produce the desired pressure distribution. At this point the design process required a theoretical tool to match an airfoil shape with the desired pressure distribution.

The Garabedian and Korn 2D, viscous computer procedure ,described in Reference 7, was selected as the tool to design an airfoil

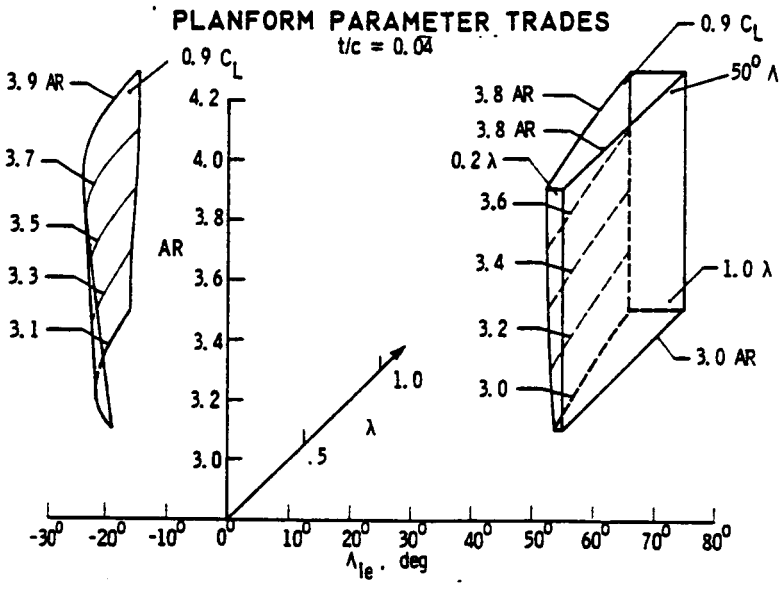

Figure 2 - Planform Parameter Trades

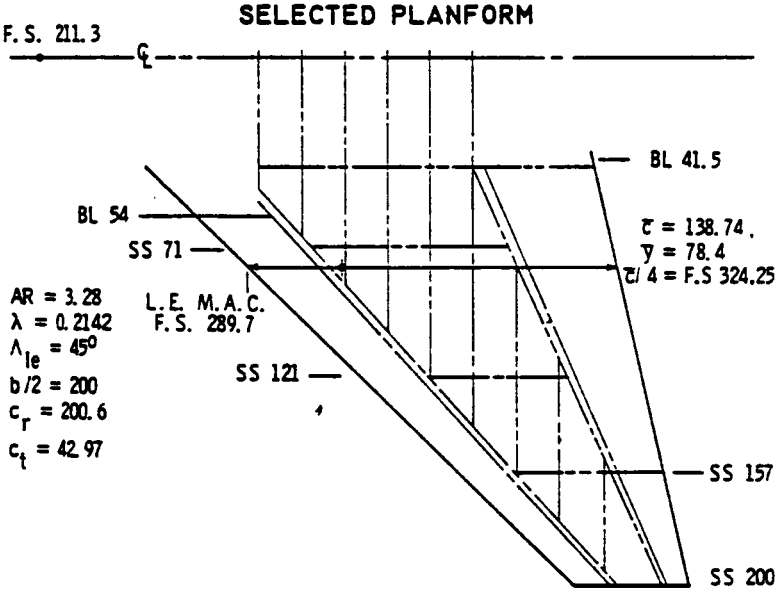

Figure 3 - Selected SMF-1 Planform

section that would produce the target pressure distribution at Mach 0.9. The joint NASA/General Dynamics design effort to define this airfoil shape is discussed in more detail in Reference 6. The selected airfoil shape and the predicted pressure distribution for this shape are shown in Figure 4 (Reference 8).

The final phase of the design process was the definition of the spanwise wing contour variation needed to align the pressure isobar's sweep angle with the local wing sweep angle. The design objective was to preserve the desired "sloped-rooftop" pressure distribution along the entire wing span. The three dimensional Jameson wing-design computer procedure described in Reference 9 was primarily used to help design the spanwise wing contour variation. The results of the Jameson procedure were used to provide design guidance to select the wing twist and airfoil camber modifications needed to align the isobar sweep with the local sweep angle.

The resulting spanwise contour variations included a nonlinear wing twist pattern and spanwise camber line variations. The selected airfoil shape was applied at the wing midspan and the required wing-root and tip-camber line modifications are shown in Figure 5. The Jameson procedure predicted that approximately 13 deg of twist was needed. This value of twist was reduced to 9.1 deg for the final SMF-1 wing design in order to reduce the anticipated supersonic penalty for such a high degree of twist.

SELECTED AIRFOIL PRESSURE DISTRIBUTION AT $C_L = .90$

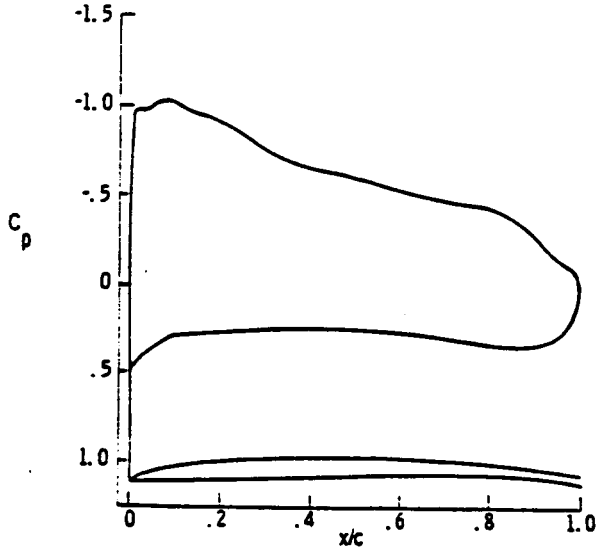

SELECTED AIRFOIL SHAPE

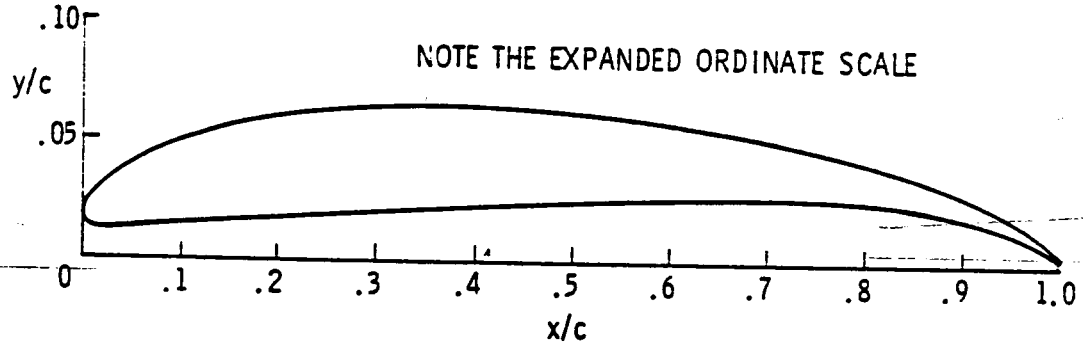

Figure 4 - Selected Airfoil Shape

SELECTED WING ROOT AND TIP CAMBER LINES

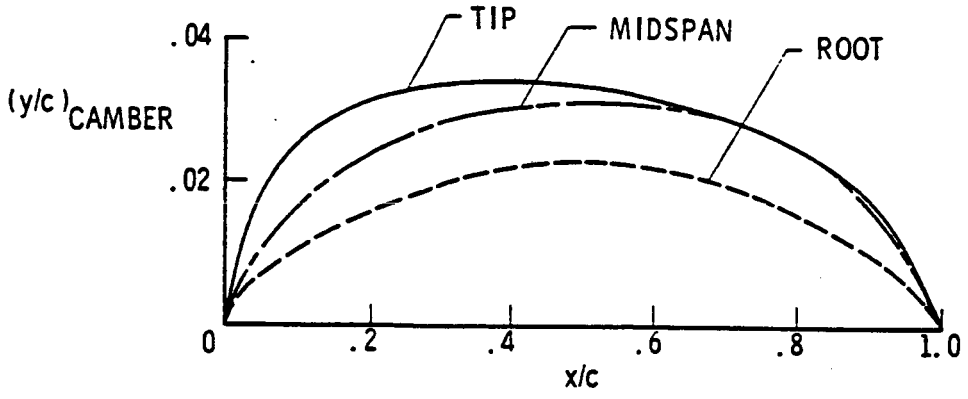

Figure 5 - Selected Wing Root and Tip Camber Lines

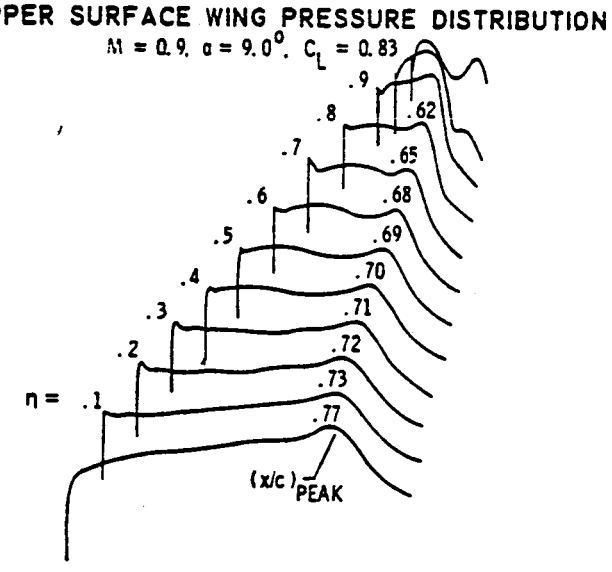

Figure 6 - Predicted Upper Surface Pressure Distribution (Jameson Procedure)

The upper-surface pressure distributions for the SMF-1 wing predicted with the 3-D Jameson procedure are shown in Figure 6. It is interesting to note that the Jameson procedure predicted more of a "flat-rooftop" pressure distribution in lieu of the desired "sloped-rooftop" distribution. The two theoretical codes used to design the SMF-1 wing were thus in disagreement over the shape of the chordwise pressure distributions. The relative success in theoretically aligning the isobars with the local sweep angle may be gauged by comparing the location of the rear pressure peak as shown in Figure 6. There was a slight tendency for the isobars to unsweep as one proceeds outboard; however, the design objective was reasonably achieved.

The problem in converting the 2-D pressure distributions into a 3-D distribution may be due to the nature of low-aspect-ratio wings. The flow over a low-aspect-ratio wing does not lend itself to a 2-D analysis as attempted on the design of the SMF-1 wing. The airfoil sections for this type of wing probably need to be totally designed with a 3-D theoretical code.

3. SMF-1 TEST RESULTS

Three test entries have been made to date with the SMF-1 wing in the Langley 8-foot transonic wind tunnel. Both force and pressure data were obtained. The significant results and aerodynamic characteristics of the SMF-1 wing are presented within this report. The initial tunnel entry (LRC-8-785) was made to determine the basic aerodynamic characteristics of the SMF-1 wing. The two subsequent entries (LRC-8-802 and LRC-8-810) were made in an attempt to improve those characteristics with vortex generators and bendable flaps and to obtain the effect of decambering the leading- and trailing-edge flaps.

The SMF-1 wing was tested on a NASA fuselage that was similar to the F-16 fuselage as seen in the model photographs in Figures 7(a), 7(b), and 7(c). The model was tested without strakes and without wing-tip missiles. The SMF-1 wing was scaled to 1/15 of its projected full-scale size. The dimensions of the wing are presented in Table 1 and compared to the previous variable-camber wing (W18).

Drag polars for the SMF-1 wing at Mach 0.60, 0.80, 0.85, 0.90, 0.92, 0.95, 0.975 and 1.20 are presented in Figures 8(a) thru 8(h). All of these polars are for the model with the horizontal tail off. At Mach numbers where comparable data exists, the polars for wing W18 are included. In Figures 9(a) and 9(b) the →go to p26

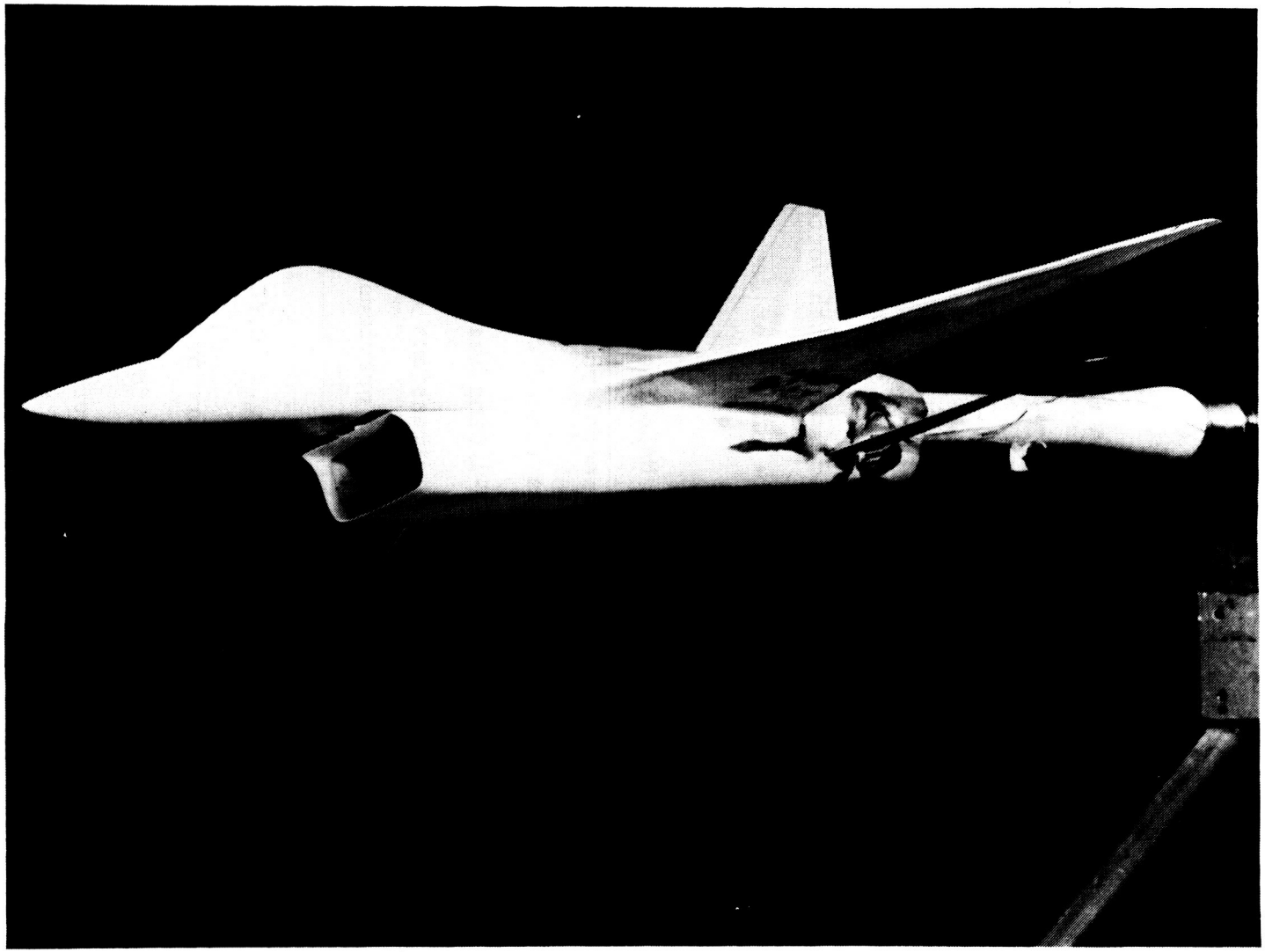

Figure 7(a) SMF-1 Wing on NASA Fuselage

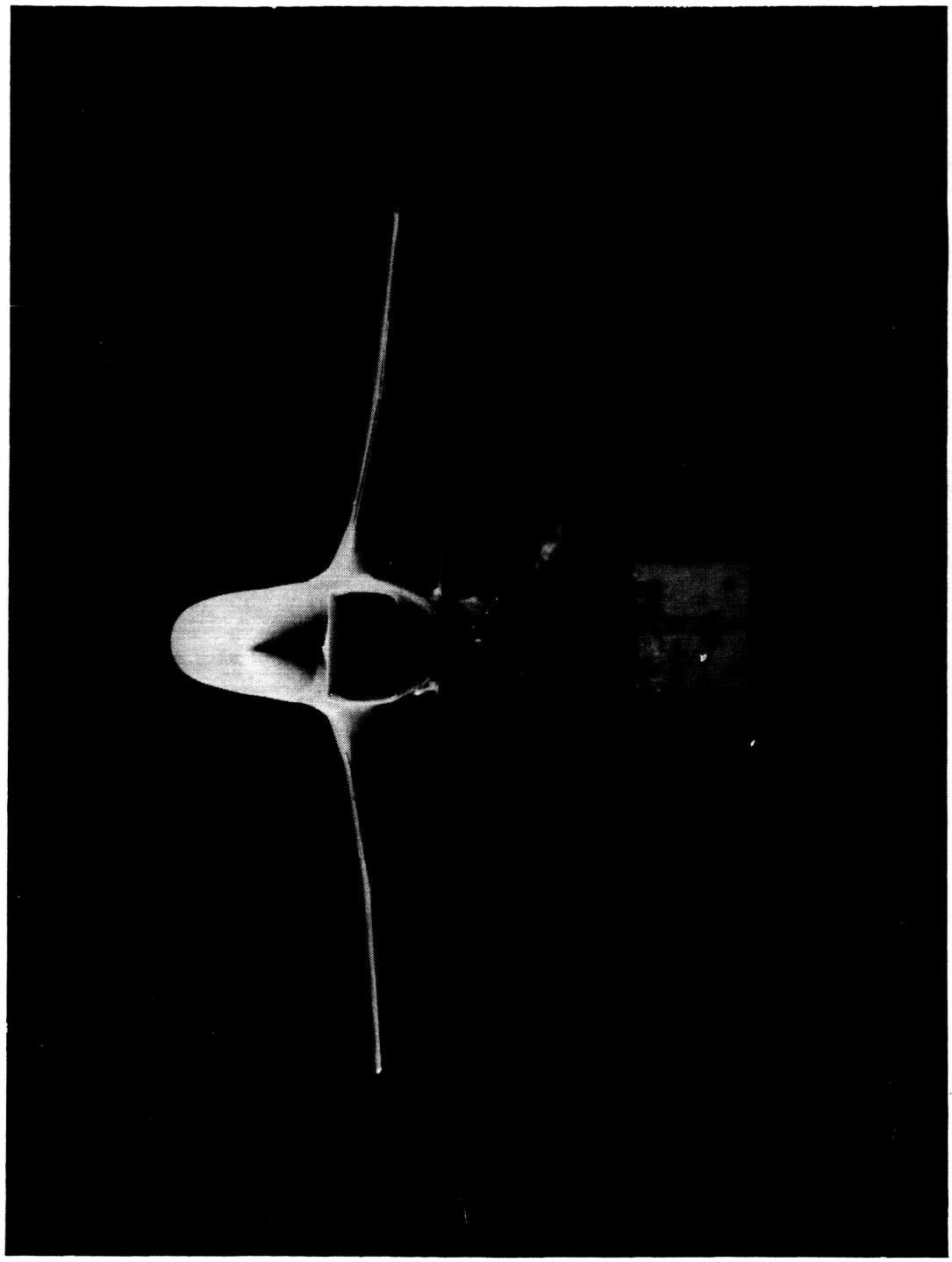

Figure 7(b) SMF-1 Wing on NASA Fuselage

Figure 7(c) SMF-1 Wing on NASA Fuselage

Span station for $\bar{c}$: $\bar{c} = 8.7564'' = 12.314 - .69775\ z_{\bar{c}}$

$z_{\bar{c}} = 5.4755''$ (z from ℄) / $\eta_{\bar{c}} = .4090$

Table 1 Comparison of SMF-1 and W18 Wings

PARAMETER	W18	W18 (1/15 scale, checks 18 NOV 79 sheet 1 in game)	SMF-1	SMF-1 (1/15 scale)	(planform)
Reference Area, S_W (FT^2)	333.3	1.4813 ✓	338.3	1.504	(1.504)
Aspect Ratio, AR	3.36	3.3606	3.28		
Taper Ratio, λ	0.2936 ✓		0.2142		
L.E. Sweep, Λ	40° ✓		45°		
Airfoil	64A0XX ✓ (design C_L base thickness form -.357 Abbott for mid notes; XX = thickness in % c — why not 04?)		Supercritical "Sloped Rooftop"		
Thickness Ratio, t/c	0.0400 ✓		0.0425		
Twist (Root-Tip) (approx)	0°-0°	+1° to -1.7° incid.	0°-9.1° (approx +2° to -8 incid)		
Dihedral	0°		0°		
Root Chord (inches-full scale), C_R	184.71	12.314 ✓ C_R	200.6	13.373	(13.3827)
Tip Chord (inches-full scale), C_T	54.24	3.616 ✓ C_t	42.97	2.865	(2.8666)
Semi-Span (inches-full scale), b/2	200.8	13.387 ✓ b/2	200.0	13.333	(13.3243)

28 June 82 W18 Trapezoid to E:

$$\lambda = \frac{C_t}{C_r} = \frac{3.616}{12.314} = .2936 = \lambda \quad \checkmark$$

$$AR = \frac{b^2}{S} \quad \frac{(2 \times 13.387)^2 \text{ in}^2}{1.4809 \text{ ft}^2 \times 144 \text{ in}^2/\text{ft}^2} = 3.361 = AR$$

both wing panels

$$S = \frac{b}{2} C_r (1+\delta) = \frac{(13.387)\text{in}\,(12.314)\text{in}\,(1+.2936)}{144 \text{ in}^2/\text{ft}^2}$$

check: $S = 2\left(\frac{b}{2}\right)\left(\frac{C_r + C_t}{2}\right) = 213.2549 \text{ in}^2 = 1.4809$ — checks their area ∴ C_r must be on E

$$S = 213.2467 \text{ in}^2 = 1.4809 \text{ ft}^2$$

psoz Ethrin Mean Aero chord

$$\bar{C} = \frac{2}{3} C_r \left(\frac{1+\delta+\delta^2}{1+\delta}\right) = \frac{2}{3}(12.314'')(1.0666) = 8.7564'' = \bar{C}$$

(1.0666 ✓)

$$c = C_r + \frac{z}{\text{span location from E}} (\tan \Lambda_{TE} - \tan \Lambda_{LE}) \Rightarrow C_t = 3.616'' = 12.314'' + 13.387''(\tan \Lambda_{TE} - \tan 40°$$

$$= 12.314 + z(\tan 10.72 - \tan 40)$$

$$C'' = 12.314 - .649735\, z \quad \checkmark \quad b/2$$

check $c = 12.314 - .649735 \times 13.387$

$= 3.616 = C_t$ checks

$$\frac{3.616 - 12.319}{13.387} + \tan 40 = \tan \Lambda_{TE}$$

.8 = T ✓ checks

$.1894 = \tan \Lambda_{TE}$ ✓

$\Lambda_{TE} = 10.$

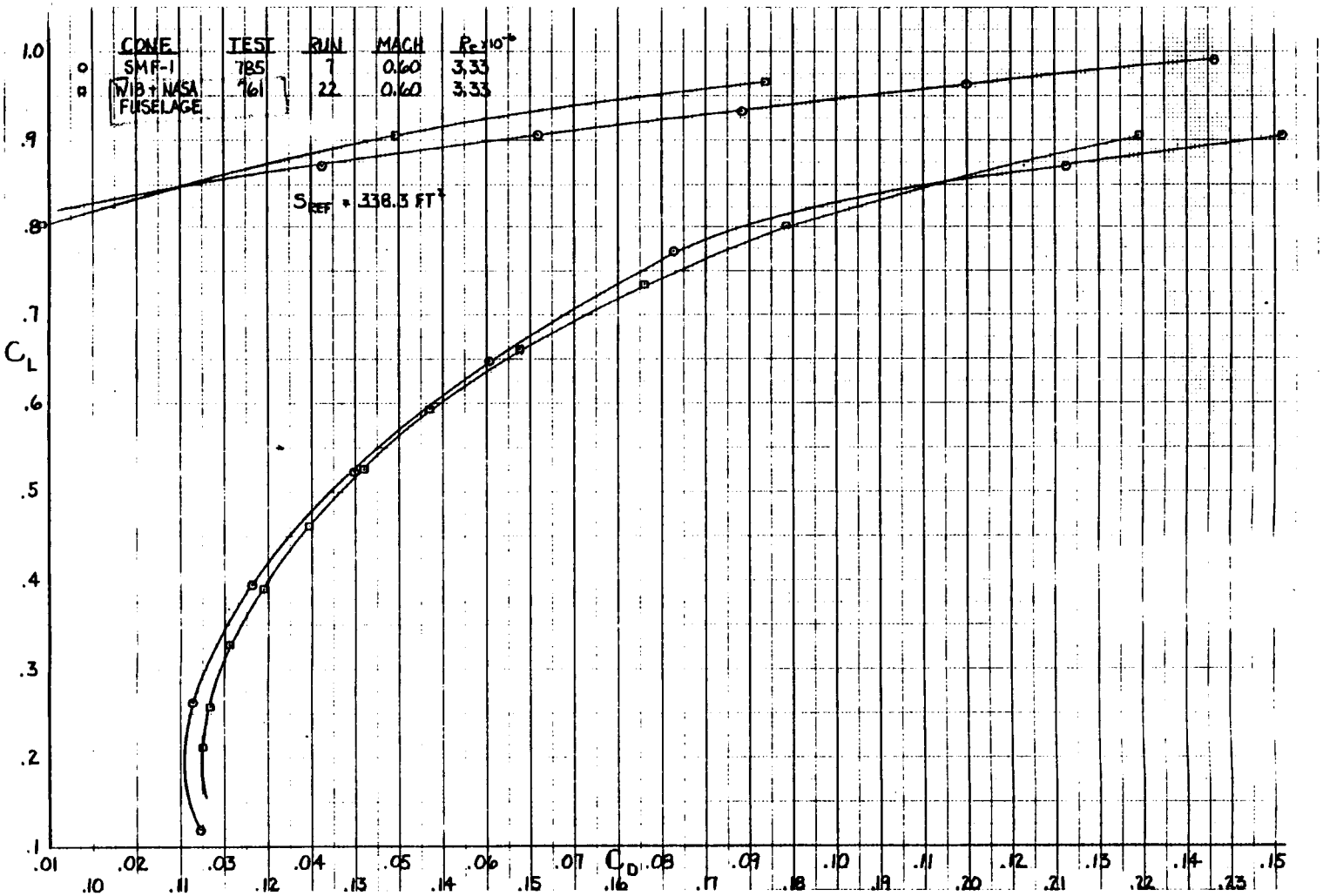

Figure 8(a) SMF-1 Drag Polar (Horizontal Tail Off), Mach = 0.60

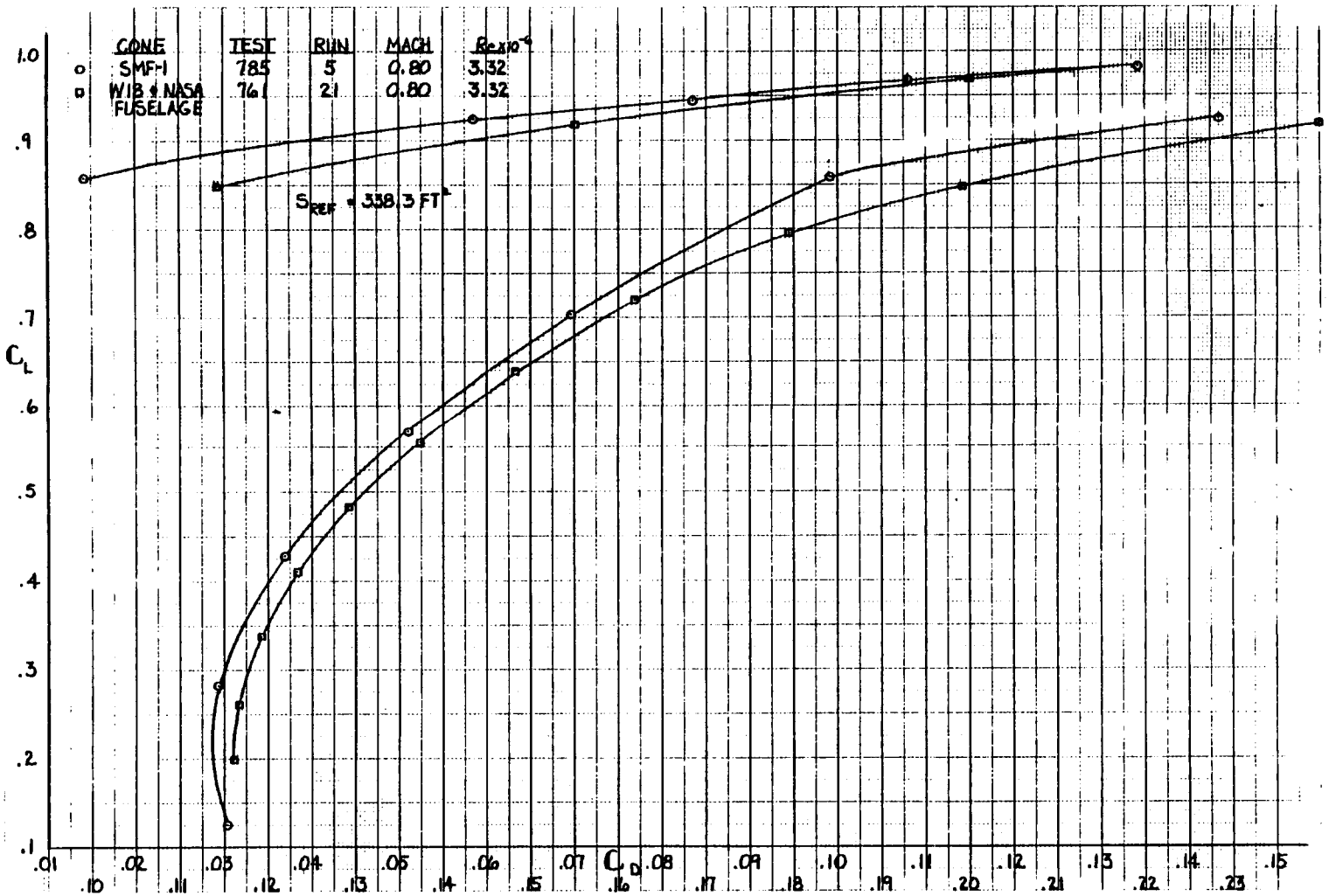

Figure 8(b) SMF-1 Drag Polar (Horizontal Tail Off), Mach = 0.80

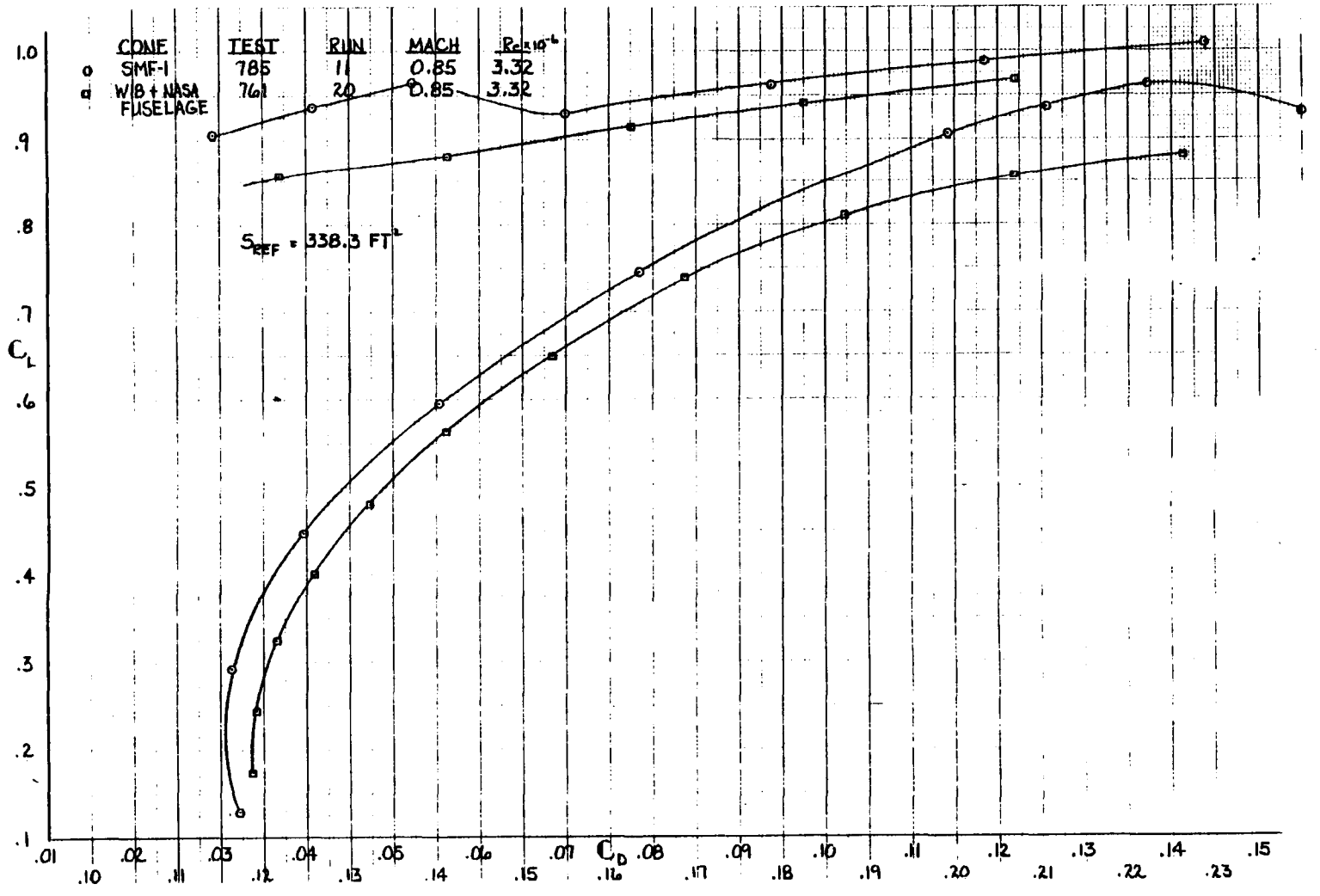

Figure 8(c) SMF-1 Drag Polar (Horizontal Tail Off), Mach = 0.85

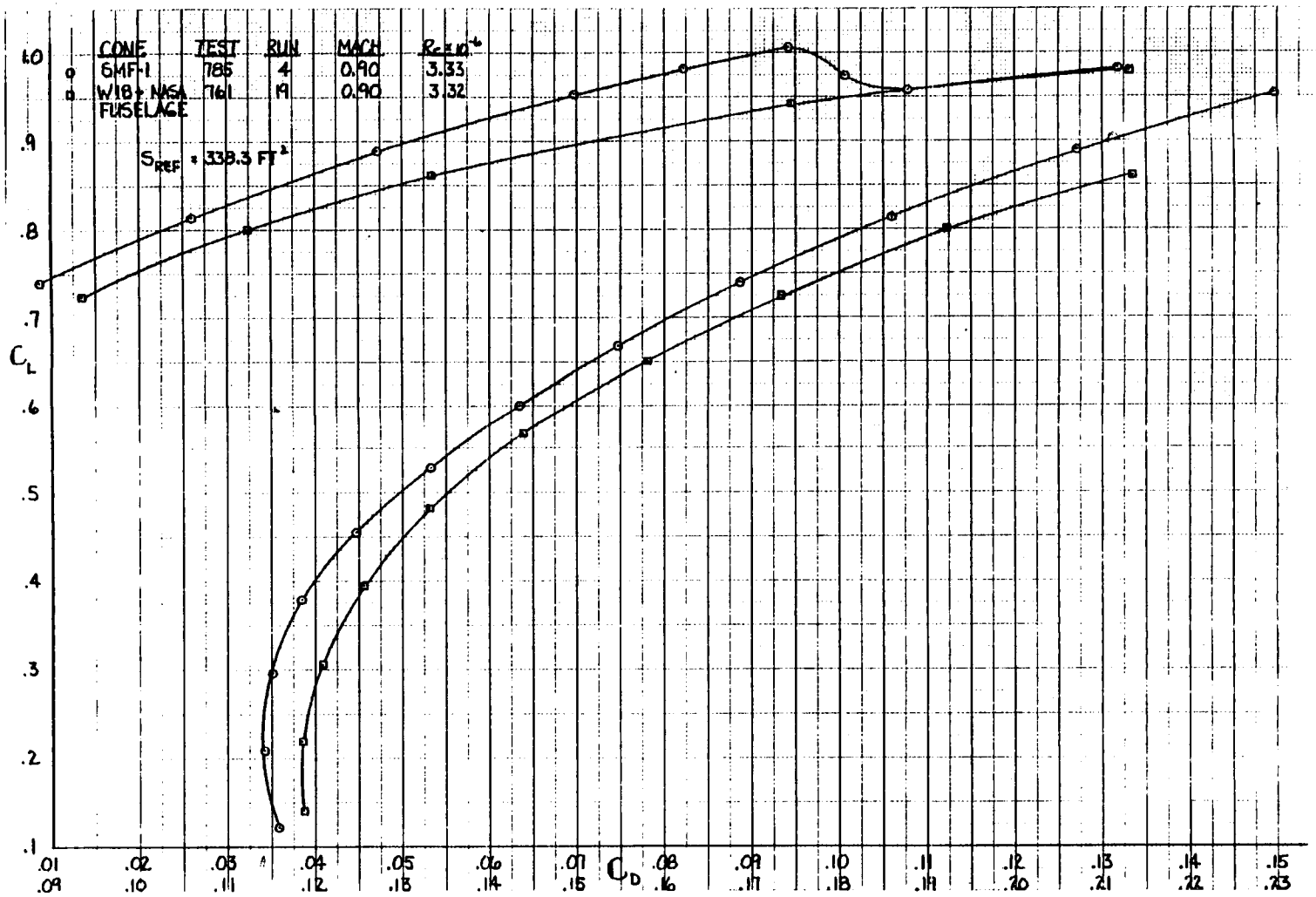

Figure 8(d) SMF-1 Drag Polar (Horizontal Tail Off), Mach = 0.90

Figure 8(e) SMF-1 Drag Polar (Horizontal Tail Off), Mach = 0.92

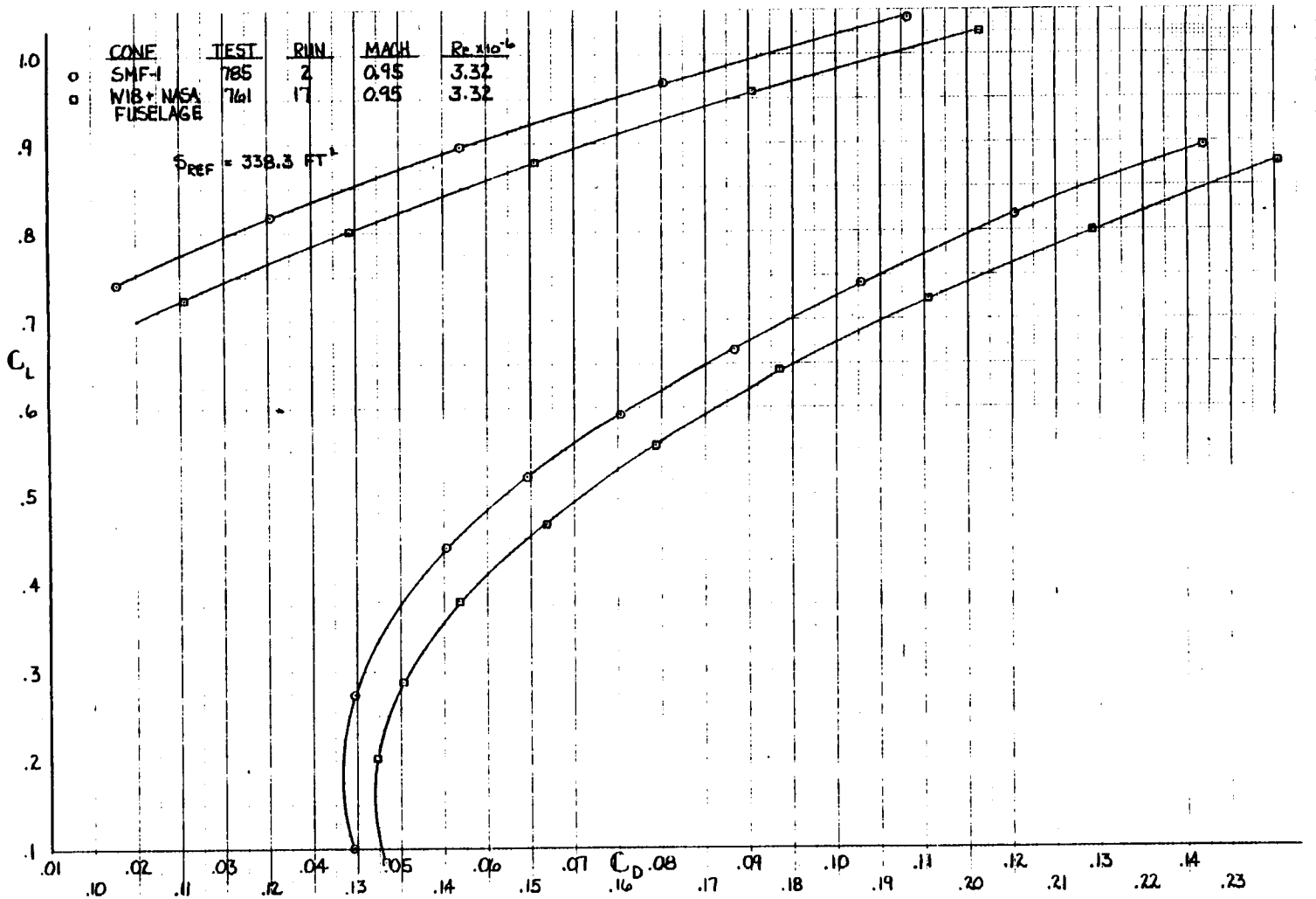

Figure 8(1) SMF-1 Drag Polar (Horizontal Tail Off), Mach = 0.95

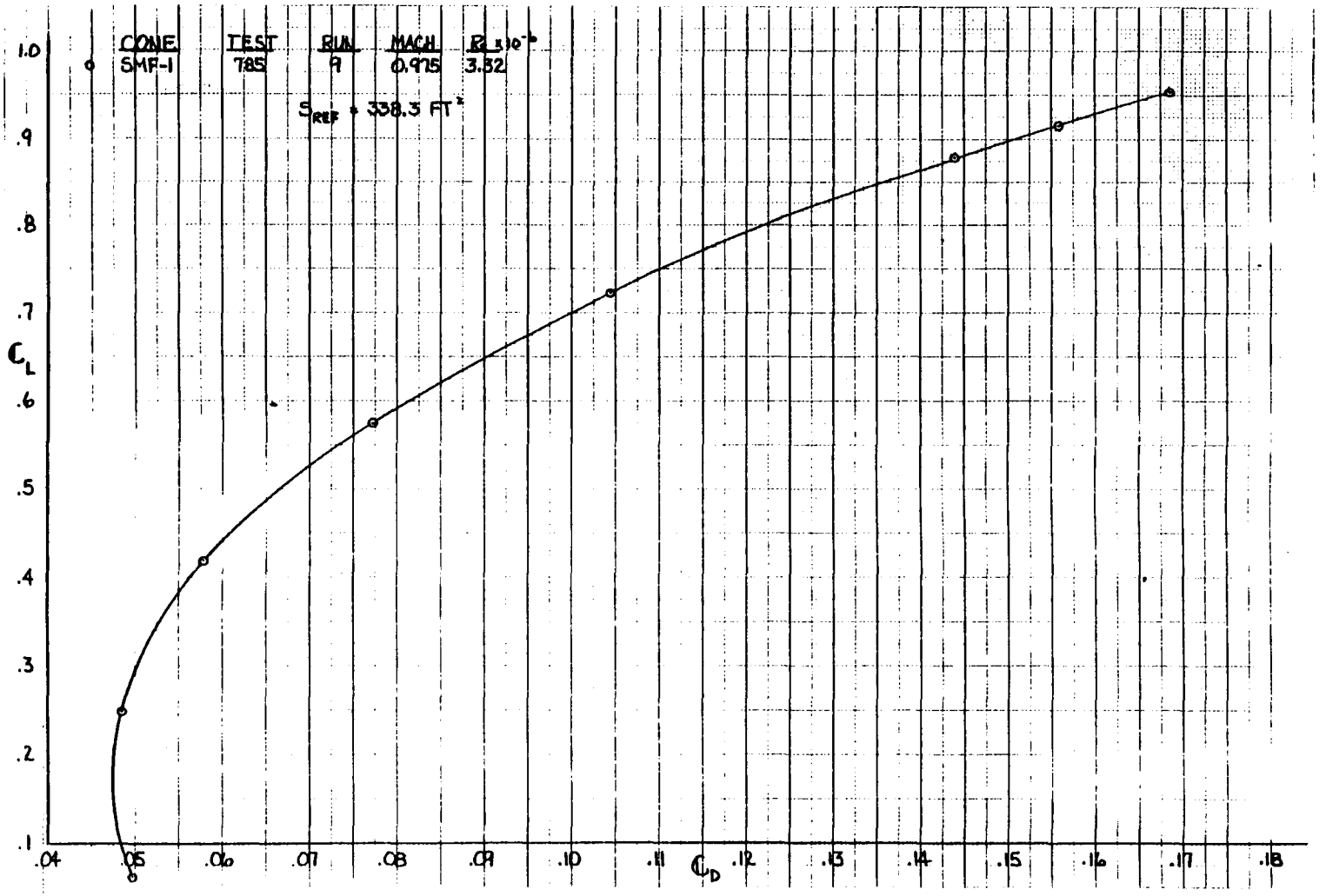

Figure 8(g) SMF-1 Drag Polar (Horizontal Tail Off), Mach = 0.975

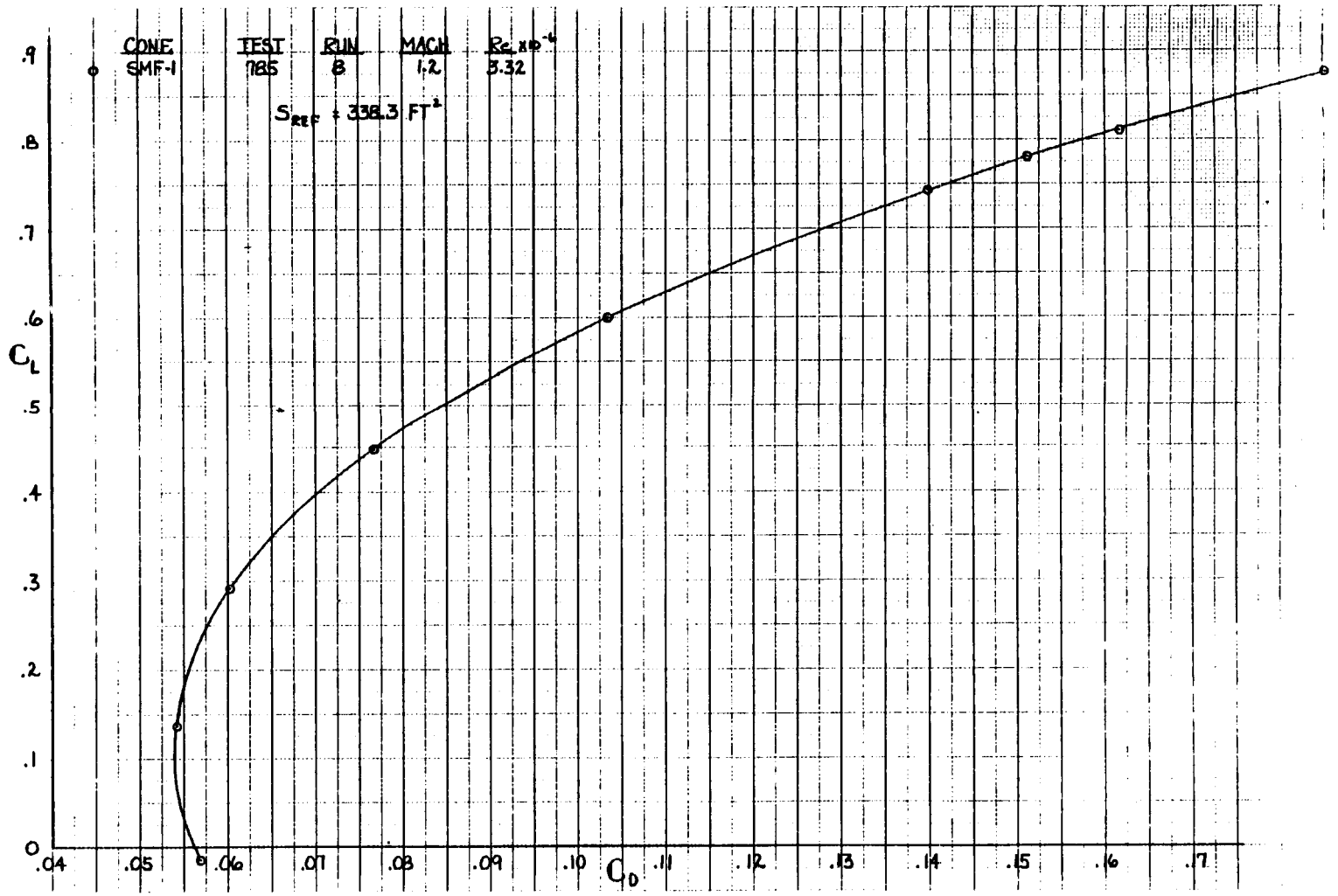

Figure 8(h) SMF-1 Drag Polar (Horizontal Tail Off), Mach = 1.20

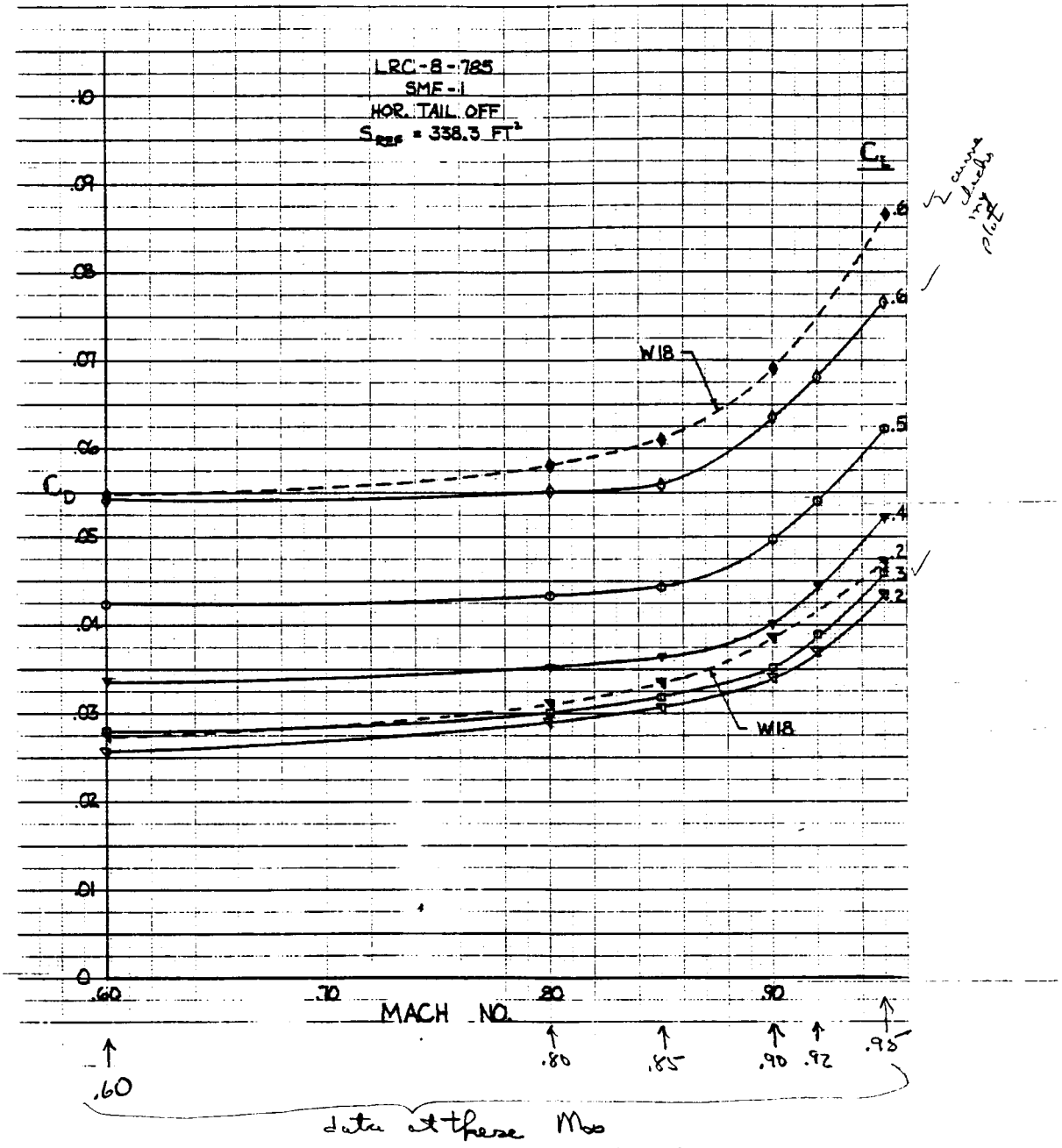

Figure 9(a) SMF-1 Drag Variation With Mach Number, Low C_L

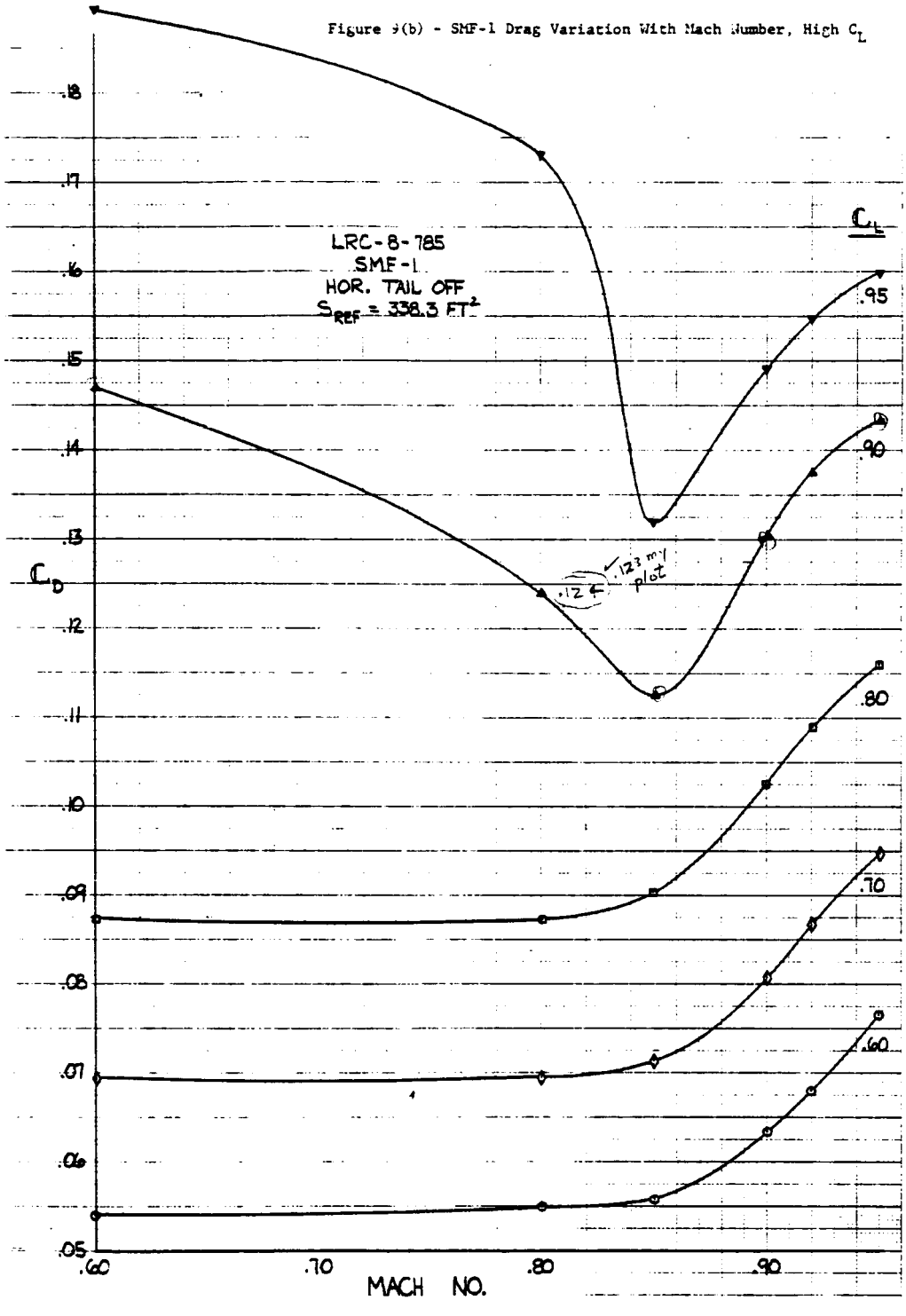

Figure 9(b) SMF-1 Drag Variation With Mach Number, High C_L

variation in drag with Mach number for the SMF-1 wing is shown at constant values of lift. The drag variations for wing W18 are included at two values of C_L for comparison. The drag of the SMF-1 configuration is consistently less than the drag of W18 at all Mach numbers tested.

Wing root bending moments were also measured on the SMF-1 wing in order that the buffet characteristics of the wing could be quantified. Bending moments for the SMF-1 wing are shown in Figure 10 as a function of C_L. The onset of buffet was defined as "the C_L where the rate of change of bending moment with lift was equal to 0.0004". This point is marked in Figure 10 and is shown as a function of Mach number in Figure 11.

The drag and buffet characteristics of the SMF-1 wing are summarized in Figure 12. The drag polar comparison between the SMF-1 wing and W18 wing is repeated to show the increment in sustained lift at the $C_{T_{MAX}}$ of the F100 engine. At this point the increase in sustained lift is 0.037 for the SMF-1 wing above W18. Wing W18 had previously been shown to generate an increase in sustained lift of 0.015 above conventional-hinged-type flaps. Therefore, the SMF-1 wing is indicating a total increment in sustained lift of 0.052 above conventional flaps, which is a 7% increase.

Also shown in Figure 12 is a comparison of the variation in drag versus Mach number between the SMF-1 wing and the W18 wing

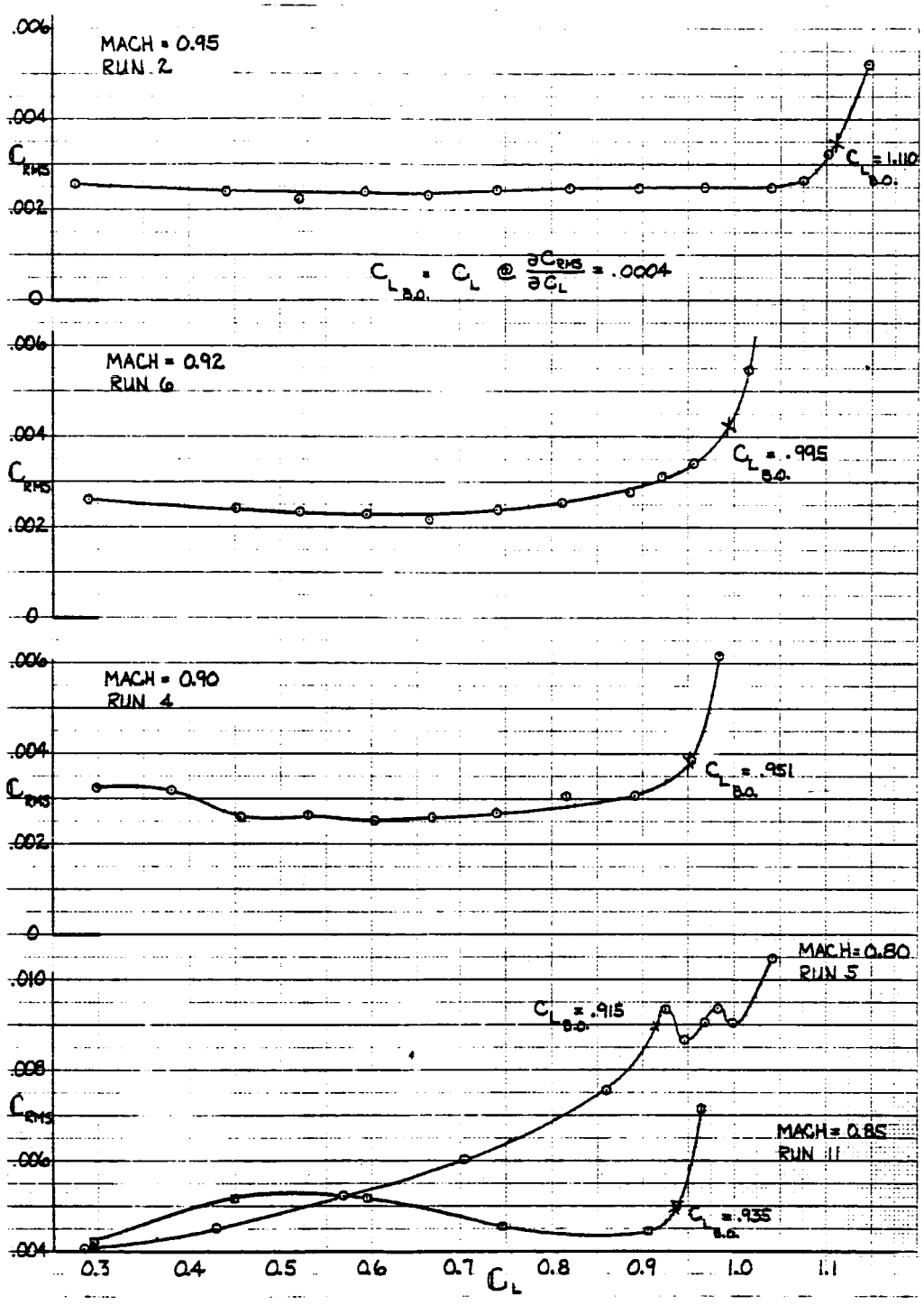

Figure 10 SMF-1 Wing Root Bending Moments

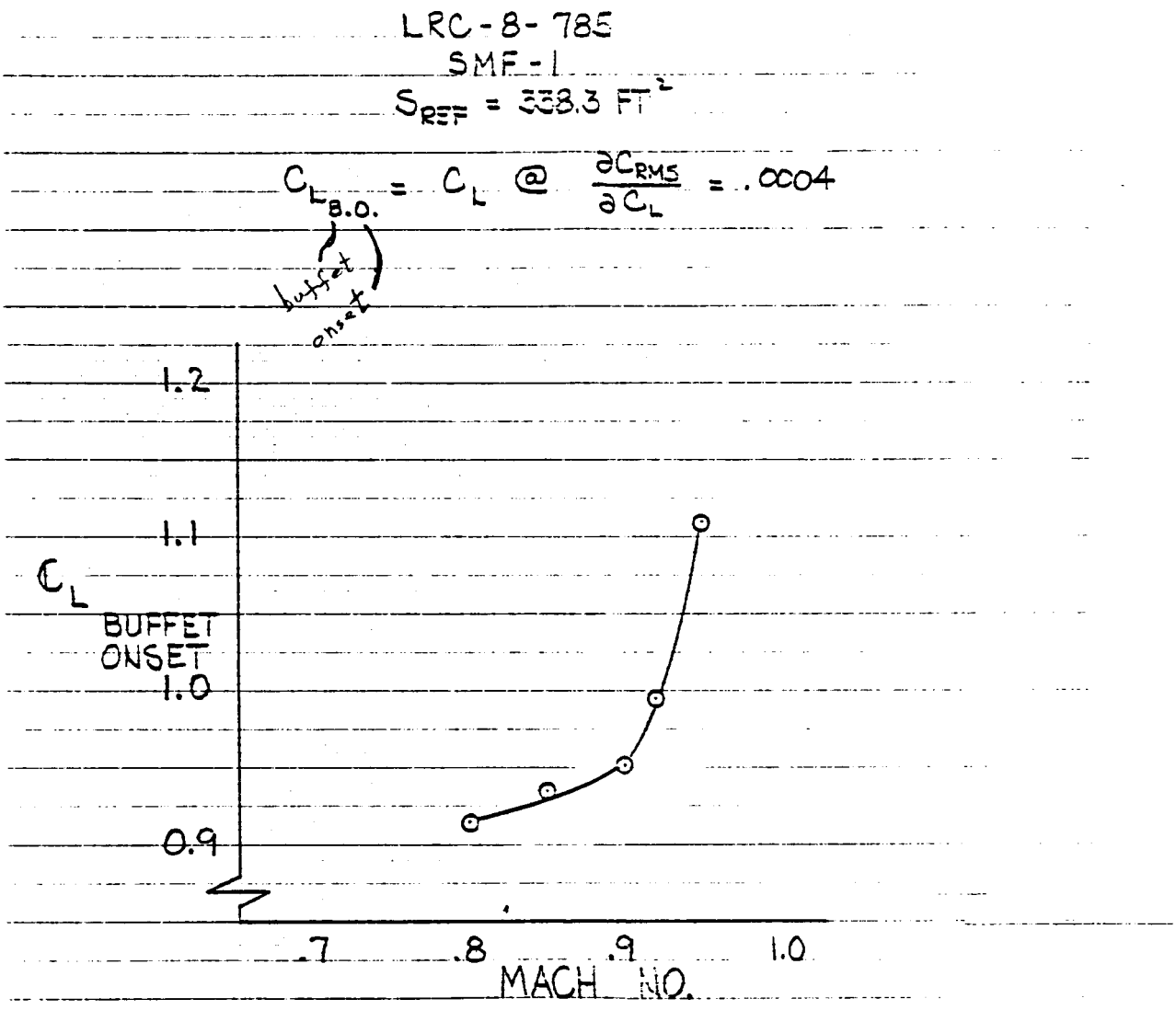

Figure 11 - SMF-1 Buffet Characteristics

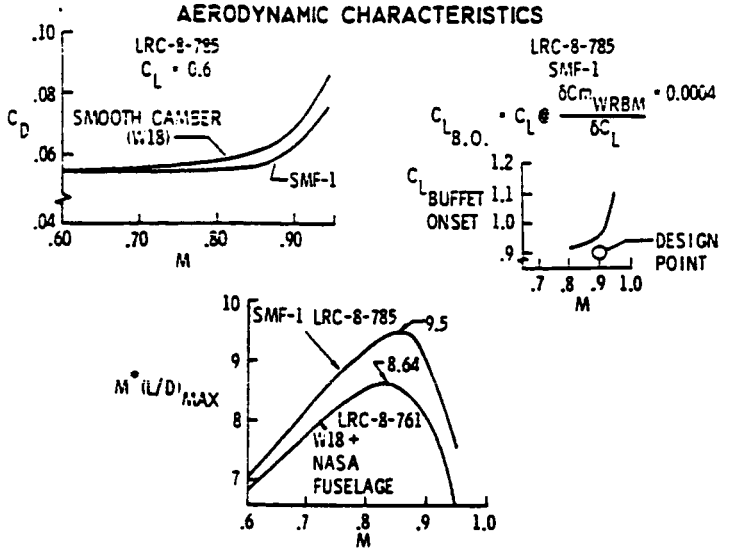

$M_\infty (L/D)_{max}$

M_∞

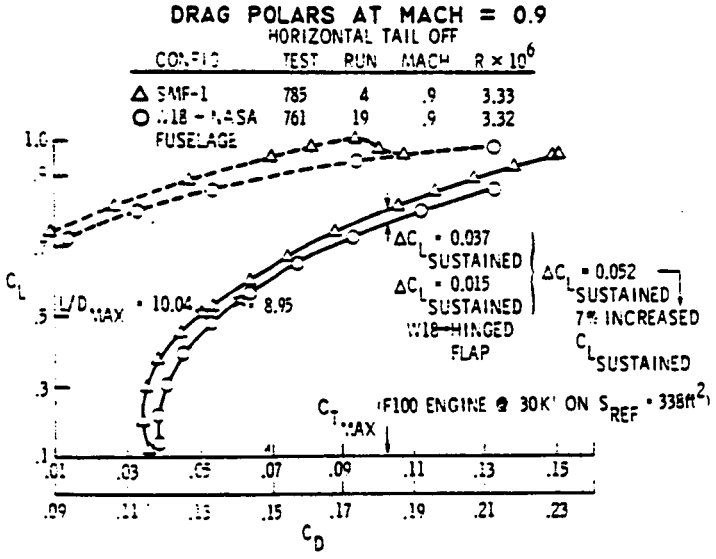

Figure 12 - SMF-1 Aerodynamic Characteristics

at $C_L = 0.60$. The drag creep or the increase in C_D at $C_L = 0.60$ between Mach = 0.60 and Mach = 0.85 is 19 counts for SMF-1 and 62 counts for W18. A lift coefficient of 0.60 was selected for this comparison because it is below the C_L where flow separation begins; yet it is high enough not to penalize either wing for their high camber. The range of Mach numbers was defined between 0.60 and 0.85 so as to avoid any drag rise as opposed to drag creep.

The lift coefficient for buffet onset is shown in Figure 12 as a function of Mach number. This is included to show that the SMF-1 wing achieved its design goal of a buffet free lift coefficient of 0.90 at Mach 0.90.

The drag difference at the design point of Mach 0.9 and a C_L of 0.9 is 211 counts between the SMF-1 and W18 wings. The large difference in drag between SMF-1 and W18 appear to be due to two primary causes. The SMF-1 wing has much less drag creep than W18 and a much higher C_L for the onset of flow separation. The onset of significant buffet signals the onset of flow separation.

The difference in the C_L for buffet onset between SMF-1 and W18 is probably due in part to the difference in their respective twists. Wing W18 did not have any twist; whereas SMF-1 had a large twist of 9.1 deg at the tip. The increased twist on SMF-1 contributes to the high values of C_L for buffet onset. These buffet results from the root-bending-moment gages were confirmed by an analysis

of the pressure data on the SMF-1 wing and by the oil flow pictures. The onset of flow separation and thus buffet can be identified from each of these sources. This data will be discussed later in the report.

The relative aerodynamic efficiency as indicated by the parameter $M(L/D)_{MAX}$ is compared in Figure 12 for the SMF-1 and W18 wings. The SMF-1 wing is seen to have a maximum value of 9.5 as opposed to 8.64 for the W18 wing.

The SMF-1 was tested with the leading- and trailing-edge flaps uncamberd to identify the drag penalty due to the camber designed into the wing box that cannot be removed with the flaps. The minimum drag of the SMF-1 wing with flaps uncambered is compared in Figure 13 with the W18 wing in its uncambered shape. Because the camber of the W18 wing was restricted to the flap region, the W18 wing, as shown in Figure 13, has all of the camber removed. As seen in Figure 13 there is approximately a 10-count penalty in minimum drag across the Mach range tested for the camber and twist in the SMF-1 wing box.

wing box camber drag penalty only ~10 counts across M. range.

As previously mentioned, pressure data were measured on the SMF-1 wing at five span stations. These data were integrated to obtain wing sectional lift coefficients. Sectional lift coefficients and leading edge pressures are shown in Figure 14 at Mach 0.90. The onset of flow separation on the wing can be identified

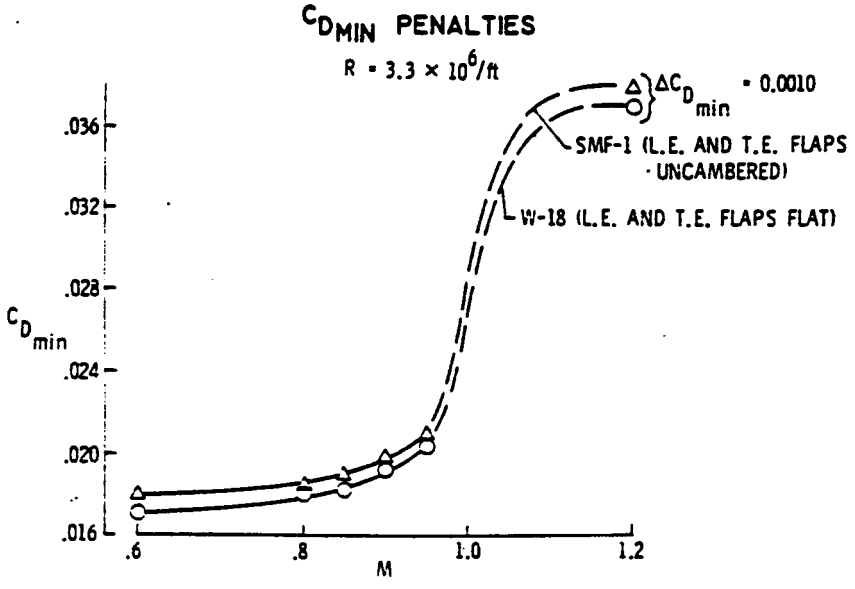

Figure 13 - Minimum Drag Penalty for SMF-1 Camber

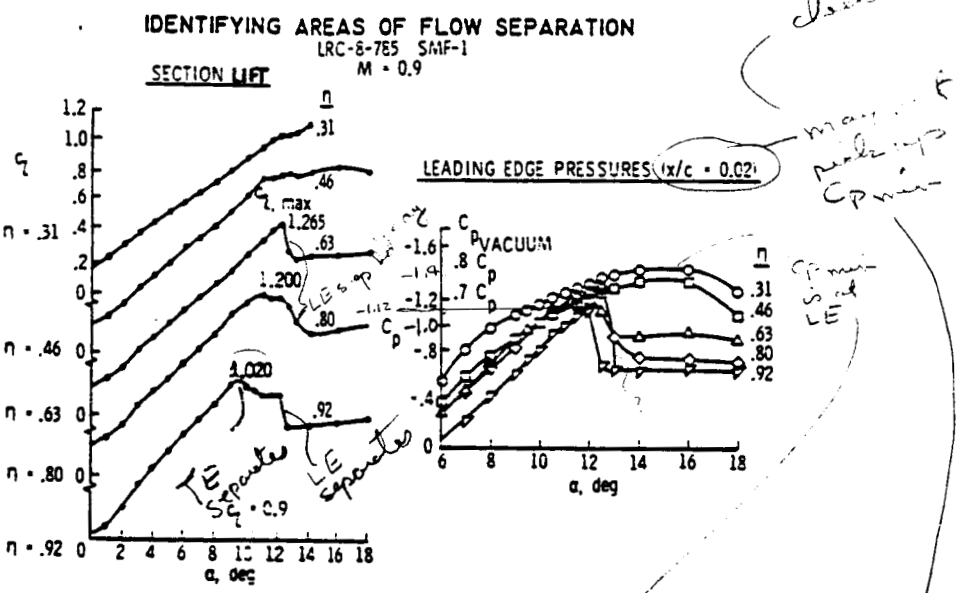

Figure 14 - Identifying Areas of Flow Separation From Pressure Data

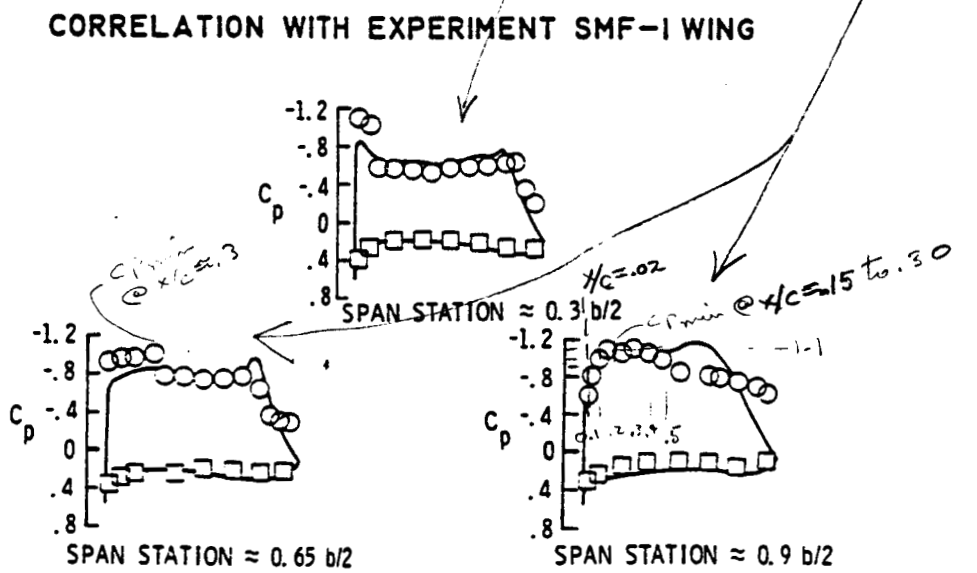

Figure 15 - SMF-1 Chordwise Pressure Distributions

in these data. A breakdown in the sectional lift coefficients is noted first in the most outboard span stations. This is the onset of flow separation on the rear portion of the wing tip. This separation was verified with the wing oil-flow photographs.

A further breakdown in the lift coefficients is noted with increasing angle of attack. This is identified as a leading-edge separation from the leading-edge pressures included in Figure 14.

Chordwise pressure data at three span locations are presented in Figure 15 for the SMF-1 wing. These data are at Mach 0.90 and a lift coefficient near the design point. The distributions as predicted by the 3-D Jameson procedure are included for comparison. The experimental distributions tend to form a "flat rooftop" distribution as predicted by the Jameson procedure instead of the desired "sloped rooftop" distribution predicted by the 2-D Garabedian and Korn procedure.

Oil flow photographs for the SMF-1 wing at Mach 0.90 for angles of attack from 6 to 14 deg are shown in Figures 16(a) thru 16(f). There is a small amount of trailing-edge separation at the lower angles of attack. As angle of attack is increased, this trailing-edge separation becomes progressively worse in the wing tip region. At the higher angles of attack it is evident that the separation in the wing tip region has moved to the leading-edge.

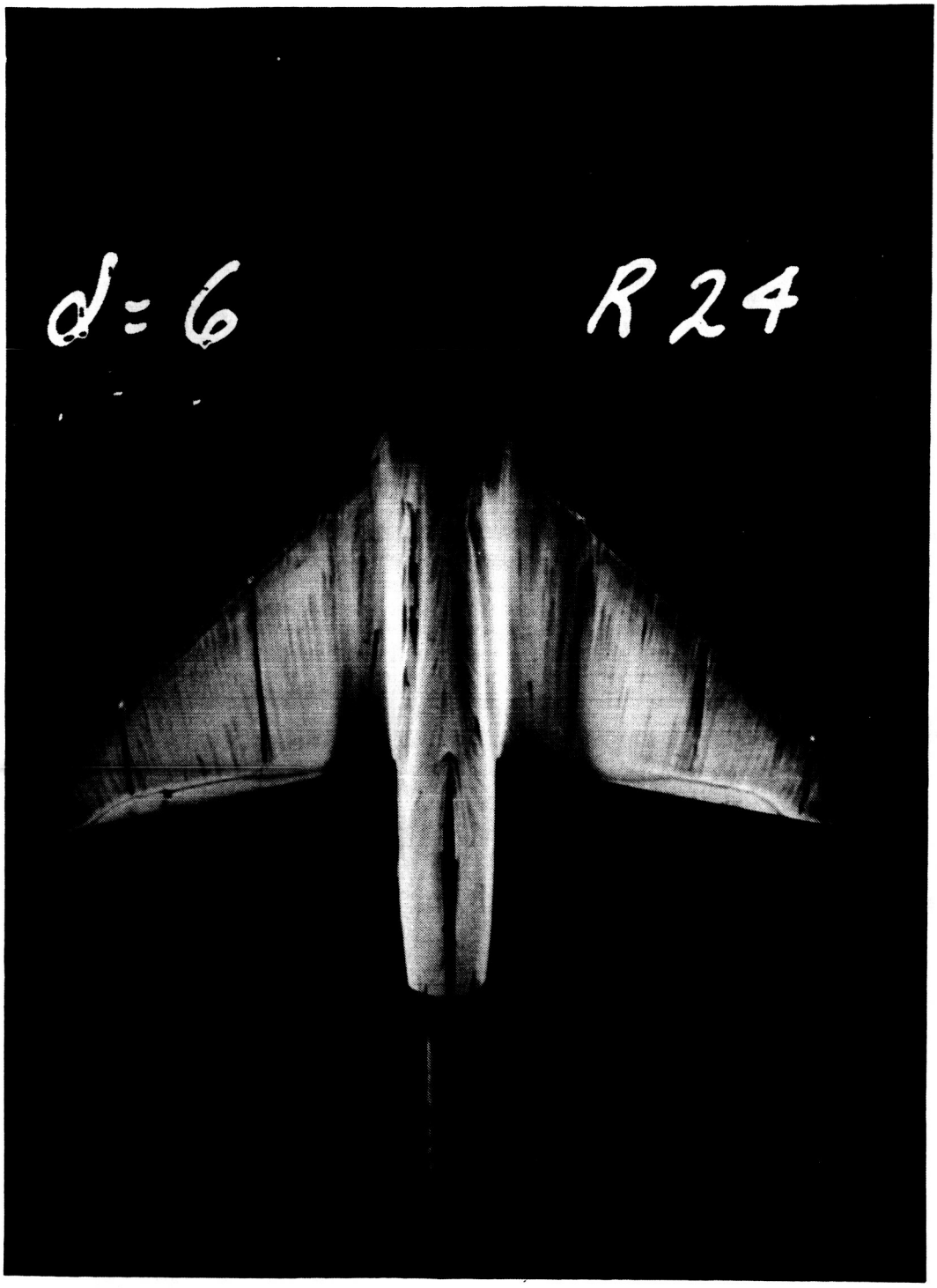

Figure 16(a) Oil Flow Photograph of SMF-1 Wing at 0.90 Mach

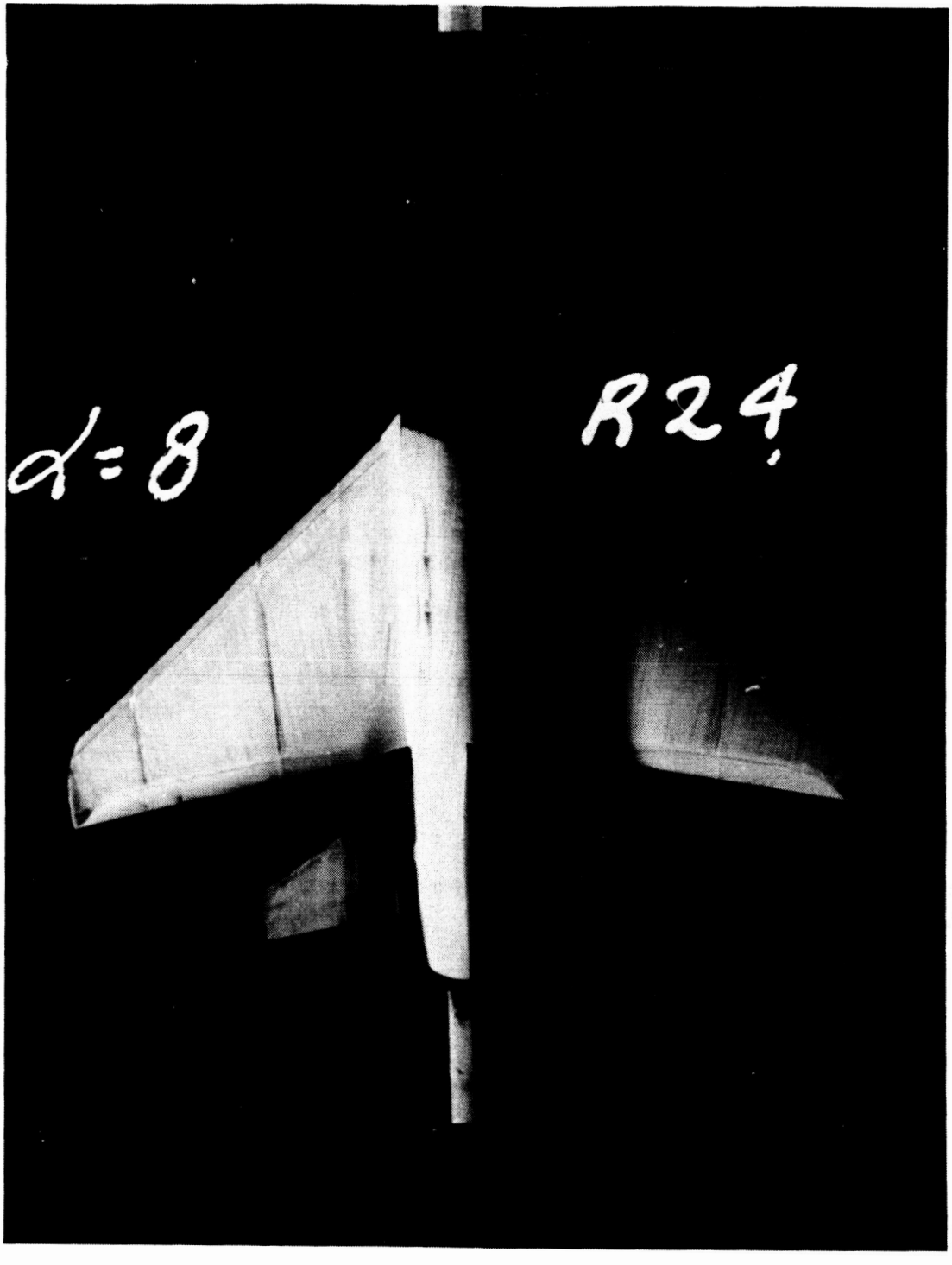

Figure 16(b) Oil Flow Photograph of SMF-1 Wing at 0.90 Mach

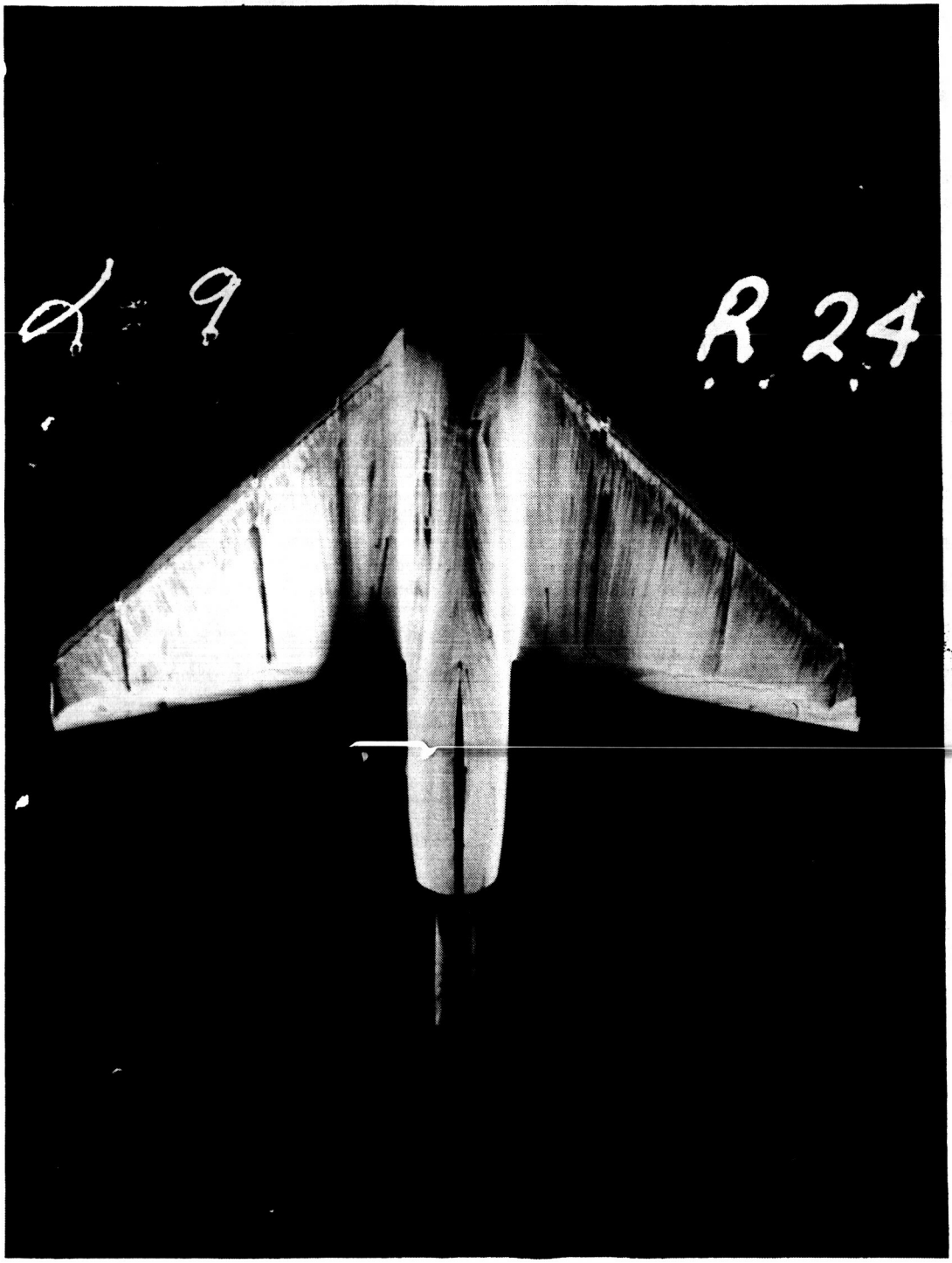

Figure 16(c) Oil Flow Photograph of SMF-1 Wing at 0.90 Mach

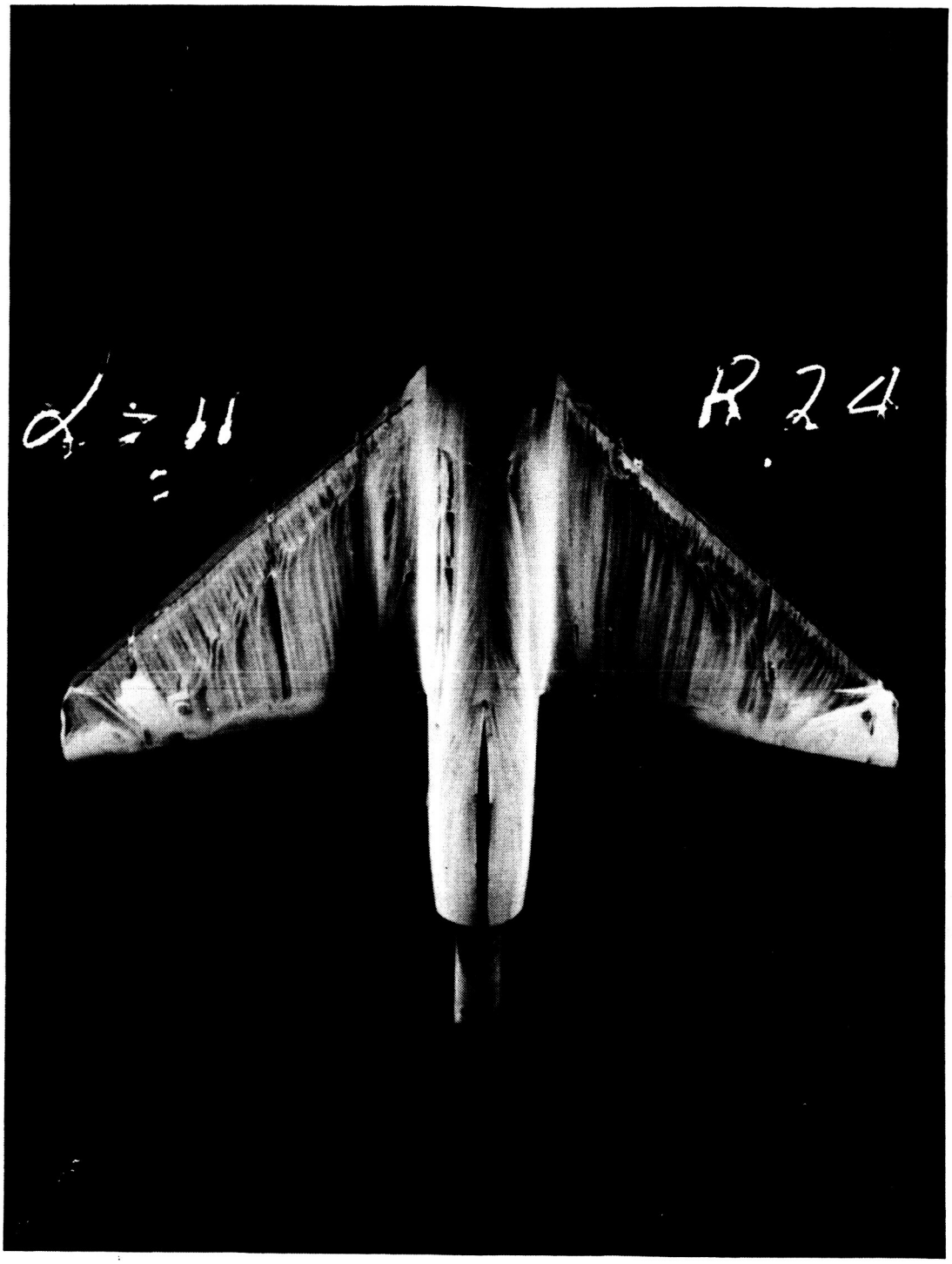

Figure 16(d) Oil Flow Photograph of SMF-1 Wing at 0.90 Mach

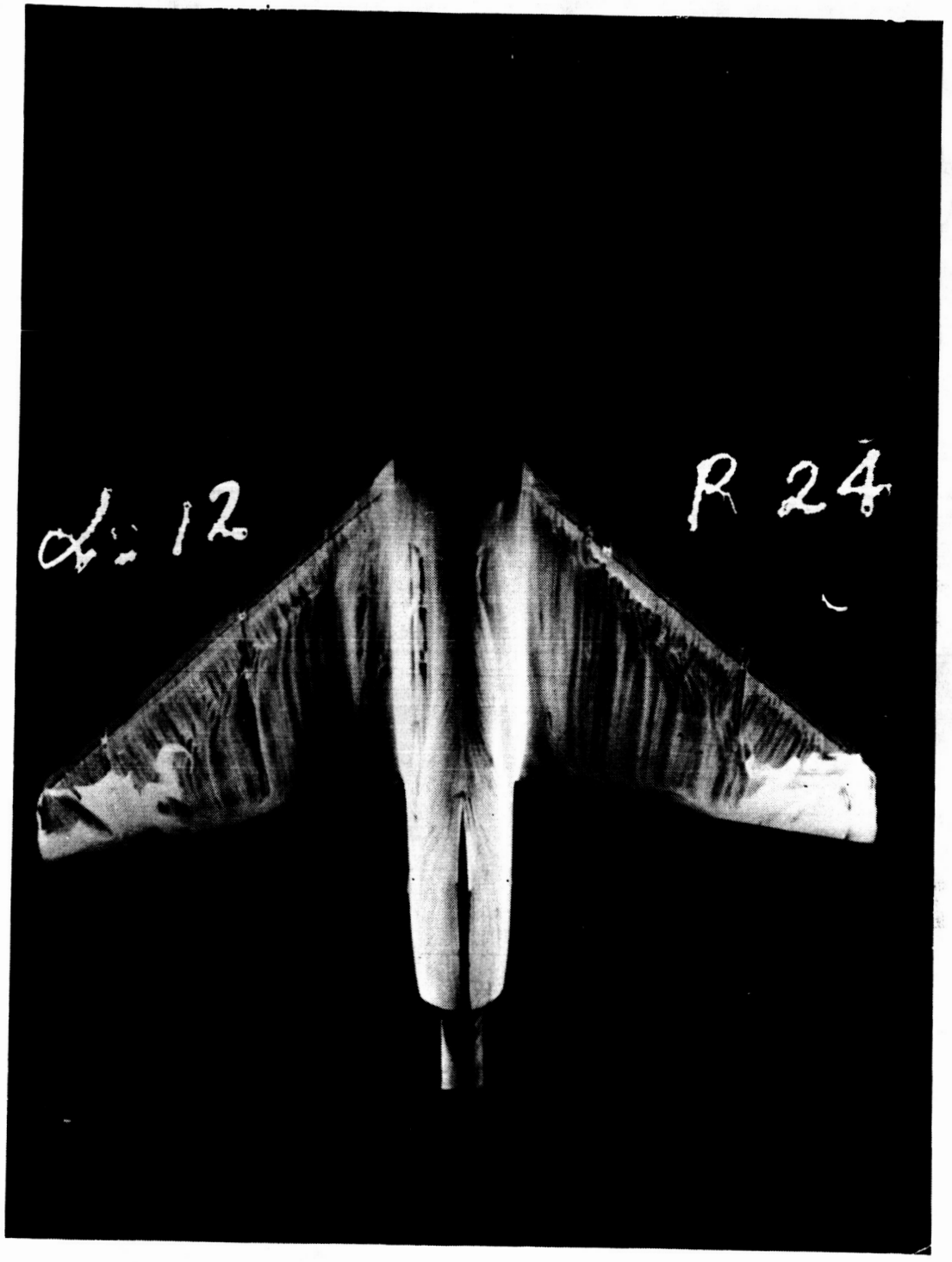

Figure 16(e) Oil Flow Photograph of SMF-1 Wing at 0.90 Mach

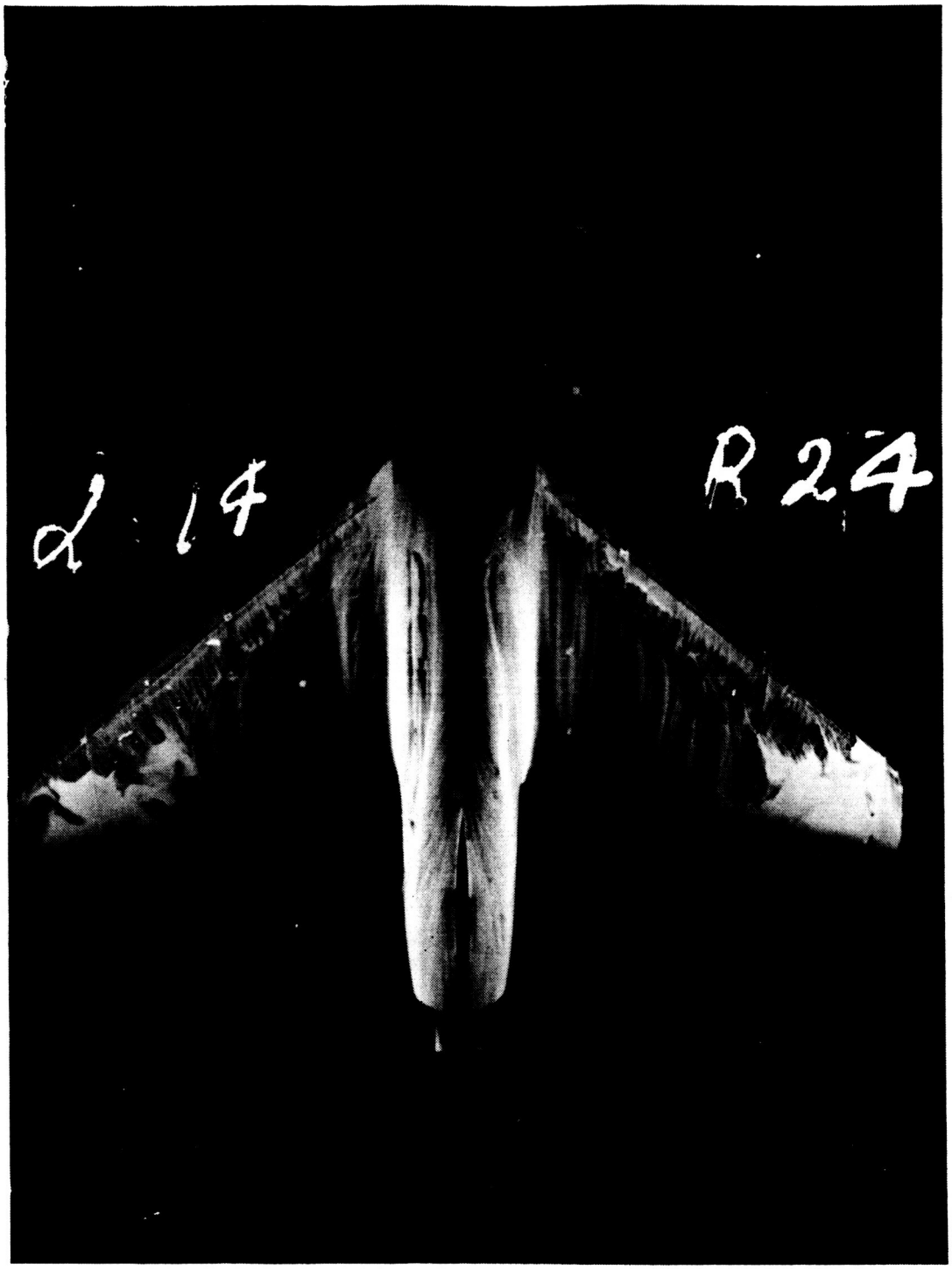

Figure 16(f) Oil Flow Photograph of SMF-1 Wing at 0.90 Mach

In subsequent tests of the SMF-1 wing several attempts were made to delay the trailing-edge separation thus further improving the wings aerodynamic characteristics. Basically these attempts involved modifying the trailing-edge camber and the addition of vortex generators to the wing's upper surface.

A set of bendable trailing-edge flaps was tested on the SMF-1 wing so that the camber shape could be "tuned" to a more desirable shape. The effect of these trailing-edge camber modifications on the SMF-1 drag polar at Mach 0.90 is shown in Figure 17. Note that at the condition corresponding to $C_{T_{MAX}}$ of the F100 engine, the camber modifications caused a loss in sustained lift. Also no improvement is found at the design lift coefficient of 0.90. At the higher C_L's some improvement is noted in the C_L for polar break.

Vortex generators on the upper wing surface were also tested on the SMF-1 wing. The size and location of these vortex generators were varied in an attempt to find a advantageous location or combination. These attempts at Mach 0.90 are shown in Figures 18(a) thru 18(c). No significant improvements were discovered.

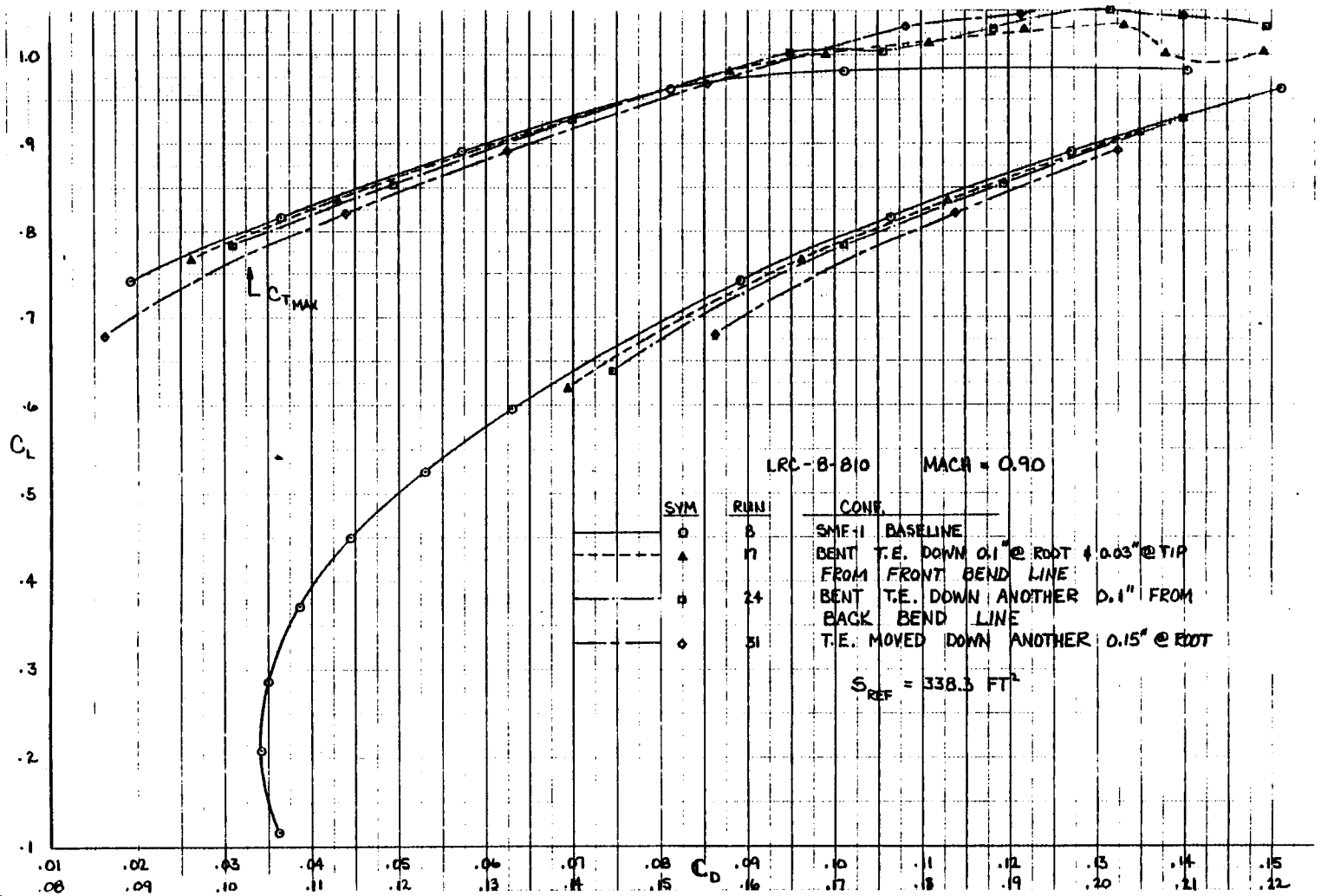

Figure 17 Effect of Modifying Trailing-Edge Camber on SMF-1 Drag Polar, Mach = 0.90

Bending TE flap down

HT off?

VG's on upper surface

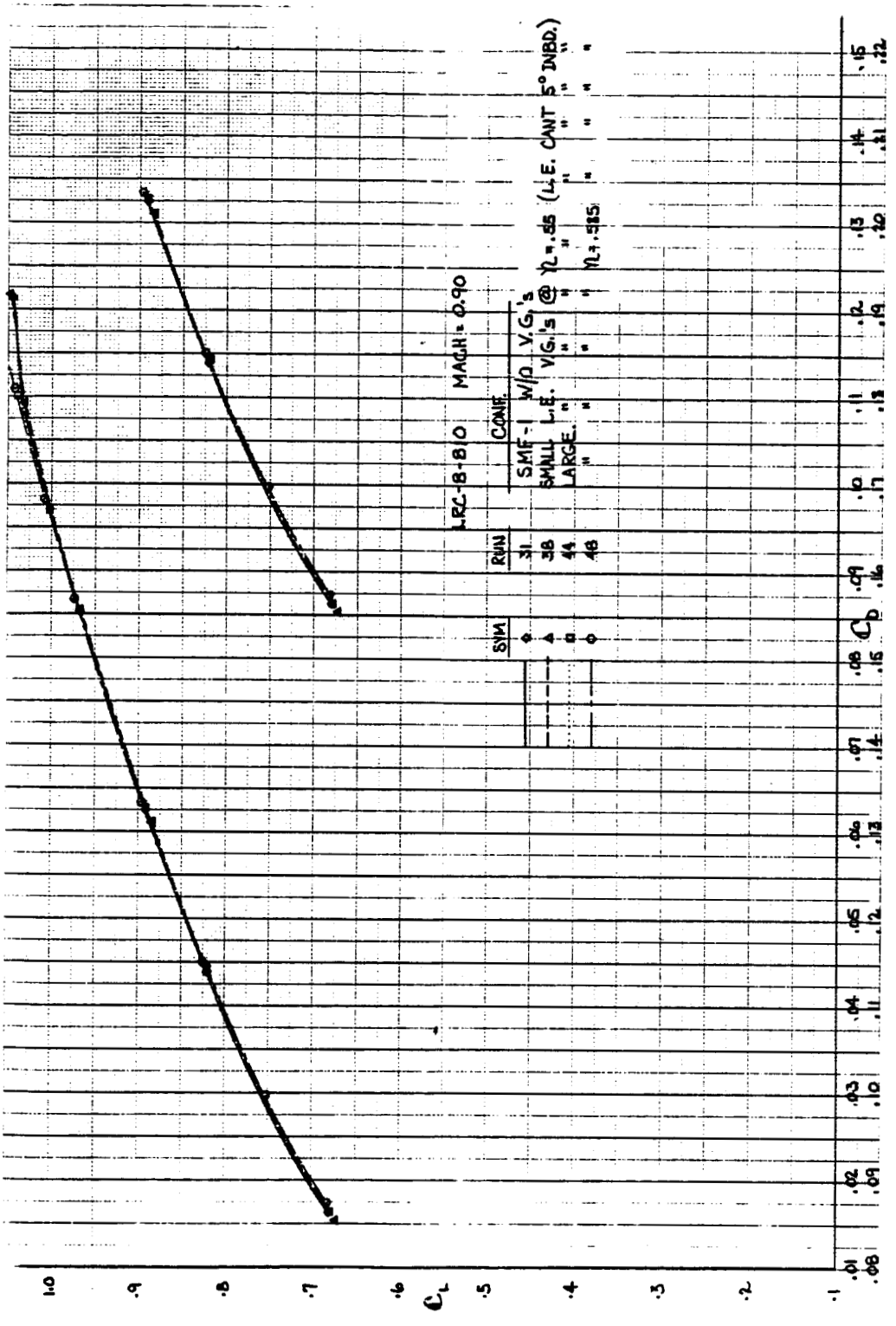

Figure 18(a) Effect of Upper Surface Vortex Generators on SMF-1 Drag Polar, Mach 0.90

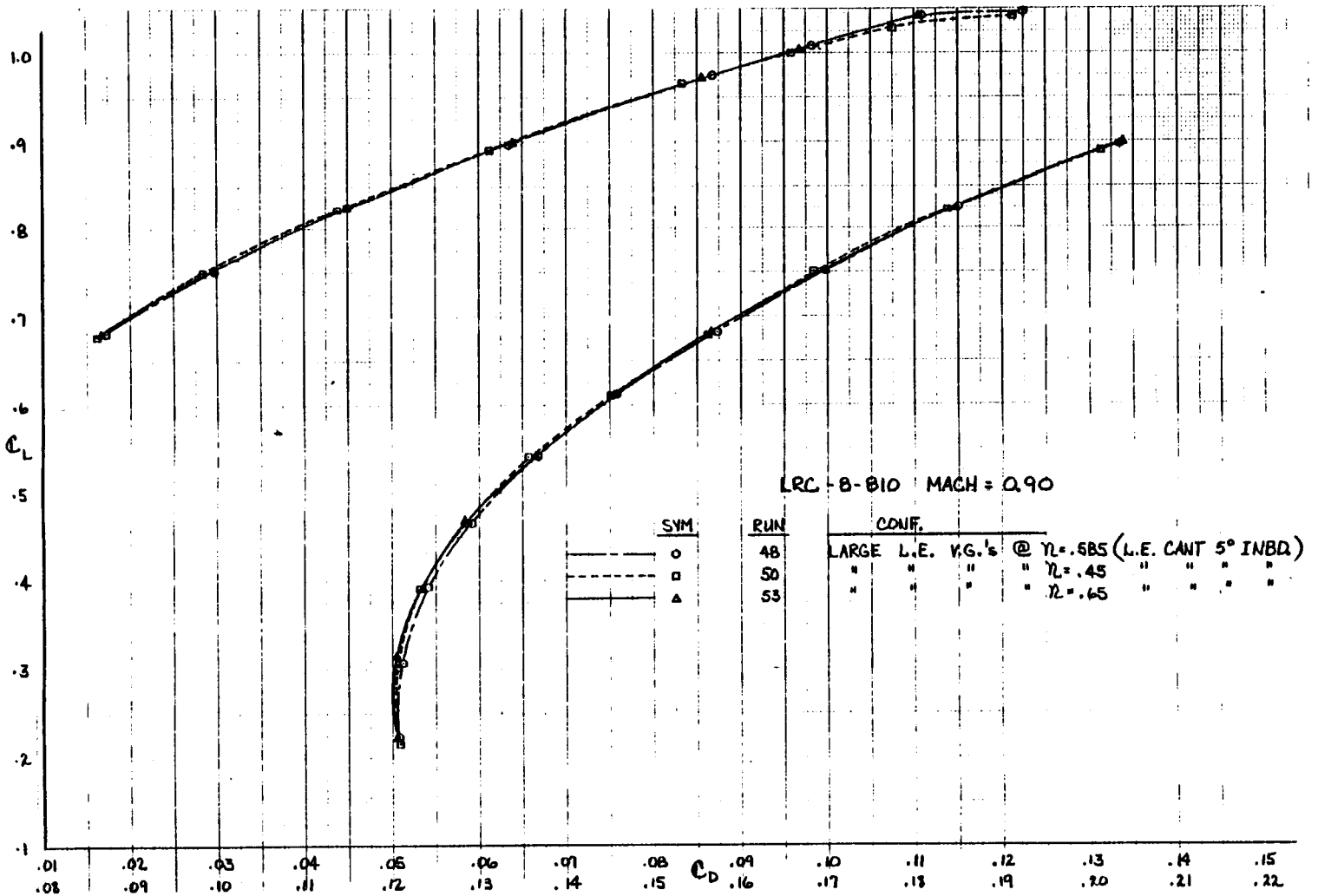

Figure 18(b) Effect of Upper Surface Vortex Generators on SMF-1 Drag Polar, Mach = 0.90

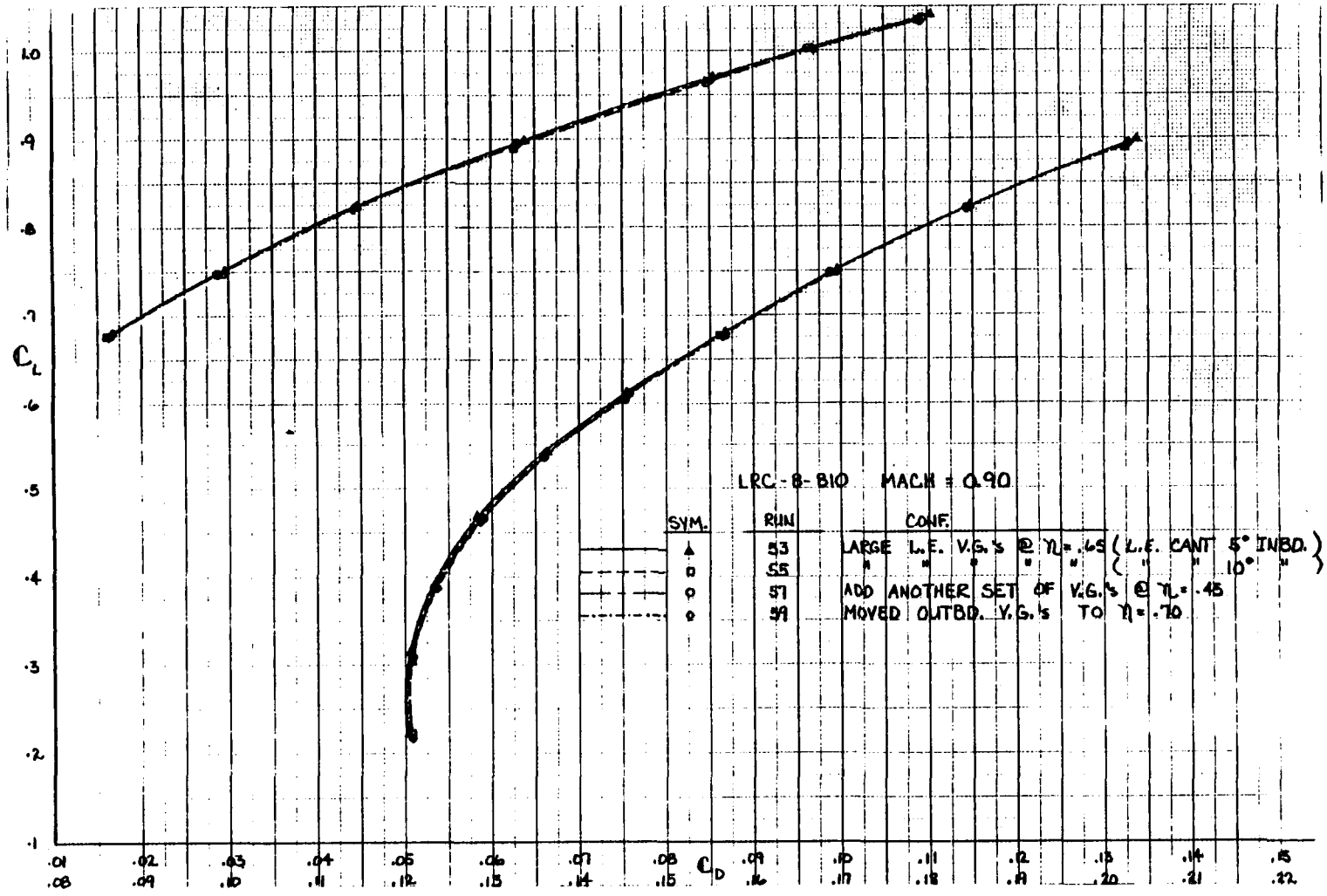

Figure 18(c) Effect of Upper Surface Vortex Generators on SMF-1 Drag Polar, Mach = 0.90

4. CONCLUSIONS

1. Significant transonic aerodynamic improvements have been demonstrated with the SMF-1 wing design. These improvements are due to the SMF-1 camber and twist combination.
2. These aerodynamics improvements in maneuver drag (7% higher C_L sustained) and cruise M $(L/D)_{max}$ (10% higher) are compelling enough to justify identifying how much of these gains can be retained by using scheduled flaps and tailored aeroelastic twist under load on the SMF-1 wing box.
3. Additional refinement of the design will probably be required to make the aerodynamic improvements compelling enough to warrant the design difficulties associated with variable camber.
4. Although the SMF-1 did produce a very successful pressure distribution, the design evolution of the SMF-1 wing did not produce a "sloped rooftop" pressure distribution. A more refined 3-D design process is apparently required to produce such a pressure distribution.
5. The flow on SMF-1 is attached up to quite high C_L's until the buffet-onset is finally induced by wing trailing-edge boundary layer separations.
6. Vortex generators and bendable flaps were used unsuccessfully in an attempt to further increase the buffet onset C_L.
7. Sufficient data were not available to separate the improvements due to twist from those due to the airfoil contour.
8. The 3-D Jameson procedure appears to be a promising tool for future design work.

5. RECOMMENDATIONS

1. How much of these gains can be retained with the use of simple leading and trailing edge flaps and aeroelastic twist with the SMF-1 wing box should be identified.
2. The SMF-1 wing should be tested on the F-16 fuselage in order to evaluate its performance relative to other advanced wings designed for application to the F-16.
3. The supersonic drag of the SMF-1 wing with optimum up-rigged flaps and reduced twist due to aeroelastic deflections should be evaluated experimentally in order to determine what, if any, supersonic penalty exists relative to other advanced wings designed for application to the F-16.
4. Further development of the theoretical wing design procedure used for the SMF-1 airfoil is warranted.
5. The aerodynamic improvements due to twist alone need to be separated from those due to airfoil shape. The optimum design should combine the improvements due to both; however, the realtive importance of the two needs to be identified.
6. The relative merits of available transonic computer codes need to be identified. This task is currently being investigated at General Dynamics, and the results will soon be published.

REFERENCES

1. Lydick, L. N., Analysis of the LRC 8-656 Variable Camber Wing Data, General Dynamics Fort Worth Division Report AIM 472, 11 November 1973. (General Dynamics Private Information)
2. Lydick, L. N., Analysis of the Variable Camber Wing Pressure Data from Test LRC 8-664, General Dynamics Fort Worth Division Report AIM 483, 7 March 1974.
3. Lydick, L. N., Application of a Variable Contour Wing to the F-16 Airplane, General Dynamics Fort Worth Division Report AIM 494, 10 May 1974. (General Dynamics Private Information)
4. Lydick, L. N., Advanced Fighter Wing Design for the Transonic Air Superiority Role, General Dynamics Fort Worth Division ERR-FW-1468, 20 December 1973.
5. Lydick, L. N. and Mann, H. W., Status Report on Development of a Varaible Contour Wing Design for Fighter Aircraft, General Dynamics Fort Worth Division Report ERR-FW-1653, 17 December 1975.
6. Hadley, S. K., Lydick, L. N. and Mann, H. W., Variable Contour, Supercritical, Thin, Fighter Wing Design for Transonic Maneuverability, General Dynamics Fort Worth Division Report ERR-FW-1740, 31 December 1976.
7. Bauer, F., Garabedian, P., Korn, D., and Jameson, A., Lecture Notes in Economics and Mathematical Systems, Supercritical Wing Sections II, New York, 1975.

8. Hadley, S.K., "Design and Validation of a High-Lift Transonic Airfoil," Presentation at Advanced Technology Airfoil Research Conference, March 7-9, 1978, Langley Research Center

9. Newman, P.A., and Davis, R.M., Input Description for Jameson's Three-Dimensional Transonic Airfoil Analysis Program, NASA TM X-71919, February 7, 1974.